PERGAMON

Solid-State Electronics 45 (2001) 893–914

SOLID-STATE ELECTRONICS

Field emission from carbon nanotubes: the first five years

Jean-Marc Bonard [a,*], Hannes Kind [b], Thomas Stöckli [c], Lars-Ola Nilsson [a]

[a] *Département de Physique, Institut de Physique Expérimentale, Ecole Polytechnique Fédérale de Lausanne, CH-1015 Lausanne EPFL, Switzerland*

[b] *Department of Chemistry, University of California, Berkeley, CA 94720, USA*

[c] *Centre Suisse d'Electronique et de Microtechnique, CH-6055 Alpnach, Switzerland*

Received 20 March 2000

Abstract

Carbon nanotubes, a novel form of carbon discovered in 1991, have been rapidly recognized as one of the most promising electron field emitters ever since the first emission experiments reported in 1995. Their potential as emitters in various devices has been amply demonstrated during the last five years, and recent developments of production techniques are likely to trigger future applications. This report reviews the state of the art of the current research on the electron field emission properties of carbon nanotubes and surveys their ability to provide single or multiple electron sources.

1. Introduction

Electron sources are omnipresent in modern society and play a central role in information display. It is often stated that conventional cathode ray tubes will soon be outclassed by plasma and liquid crystal displays and that the reign of electron sources is waning rapidly. Conversely, electron field emitters are now becoming increasingly attractive for similar applications. This resurgence is largely due to the recent development of cheap and robust field emitting materials.

Although field emission devices based on microfabricated Mo tips are commercially available, researchers are actively looking for alternative materials. How would the ideal field emitter look like? It should be very long and very thin, made of conductive material with high mechanical strength, be robust, and cheap and easy to process.

Imagine taking a sheet of graphite, a simple planar assembly of carbon atoms disposed in a honeycomb lattice, and rolling it up to form a cylinder. You would obtain a very long, yet very thin cylindrical object. It would have properties similar to those of graphite, be flexible but very hard to stretch. You could assemble these cylinders together in ropes, or nest several of them, with increasing diameters, like a Russian doll.

Since 1991, the dream of fabricating, manipulating, characterizing and modifying such cylindrical graphitic structures has become true. These objects were named carbon nanotubes and arose to one of the most fascinating materials that have been discovered in recent years [1]. Nanotubes show exceptional electronic [2–5] and mechanical [6–11] properties that have triggered an ever stronger effort towards applications. The possibilities are varied and promising and range from nanotube composite materials [12,13], nanoelectronics [14–16], scanning microscope probes [17,18], chemical [19] and/or biological sensors [20,21], to electron sources.

The power of carbon nanotubes as electron field emitters was already apparent from the first articles reporting extremely low turn-on fields and high current densities in 1995 [22–24]. Only a few studies followed during the next two years. From 1998 on, the perspective to use nanotubes in field emission devices spurred efforts worldwide: a first crude display as well as a lighting element were presented. Later studies addressed issues of large scale production compatible with microfabrication

* Corresponding author. Tel.: +41-21-693-4410; fax: +41-21-693-3604.

E-mail address: jean-marc.bonard@epfl.ch (J.-M. Bonard).
http://ipewww.epfl.ch/nanotubes.htm

0038-1101/01/$ - see front matter
PII: S0038-1101(00)00213-6

technology and strove towards better understanding of the emission mechanism.

This article surveys the results obtained during the first five years of activity in the field emission properties of carbon nanotubes. First, we will introduce some basics on carbon nanotubes and focus then on their electronic properties. Section 3 is devoted to the production of nanotubes since this is an essential and difficult step for the realization of an emitter. Emission results are discussed in Sections 4–6, namely film emitters, single emitters, and field emission devices.

2. Carbon nanotubes

What follows here is a short overview of the structural and electronic properties of nanotubes. The interested reader may consult recent review articles [25–28] and books [29–31] encompassing the subject.

In the ideal case, a carbon nanotube consists of either one cylindrical graphene sheet (single-wall nanotube (SWNT)) or of several nested cylinders with an interlayer spacing of 0.34–0.36 nm that is close to the typical spacing of turbostratic graphite (multiwall nanotube (MWNT)). There are many possibilities to form a cylinder with a graphene sheet [3] and only a few configurations are shown in Fig. 1. One can roll up the sheet along one of the symmetry axis: this gives either a zig-zag tube (Fig. 1(a)) or an armchair tube (Fig. 1(b)). It is also possible to roll up the sheet in a direction that differs from a symmetry axis: one obtains a chiral nanotube (Fig. 1(c)), in which the equivalent atoms of each unit cell are aligned on a spiral. Besides the chiral angle, the circumference of the cylinder can also be varied. In general, the whole family of nanotubes is classified as zig-zag, armchair, and chiral tubes of different diameters. The MWNT of Fig. 1(d) is made of four SWNTs of increasing diameter with a layer spacing of 0.34 nm.

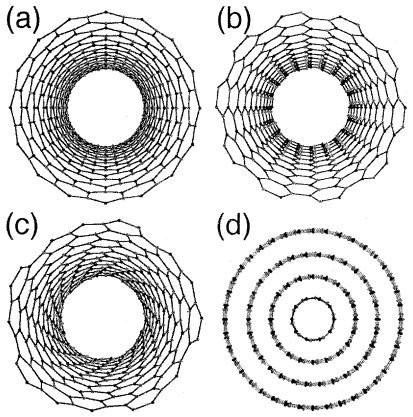

Fig. 1. Models of different nanotube structures. (a)–(c) are SWNTs of 1.25 nm diameter of (a) zig-zag, (b) armchair, and (c) chiral type. (d) represents a MWNT formed by four armchair tubes of increasing diameter with an interlayer separation of 0.34 nm. The image has been reduced by a factor of 2 with respect to images (a)–(c). The images have been generated with the software Mathematica 4.0 using a notebook by Brandbyge [197] that allows one to draw the structure as well as to compute the energy bands of SWNTs.

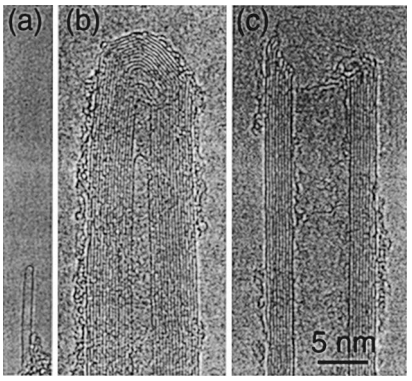

Fig. 2. TEM pictures of the ends of (a) a SWNT, (b) a closed MWNT, and (c) an open MWNT. Each black line corresponds to one graphene sheet viewed edge-on. The micrographs are reproduced at the same magnification.

This diversity of possible configurations is indeed found in practice, and no particular type is preferentially formed. In most cases, the layers of MWNTs are chiral [1,32] and of different helicities [33]. The lengths of SWNTs and MWNTs are usually well over 1 μm and diameters range from ~1 nm (for SWNTs) to ~50 nm (for MWNTs). Pristine SWNTs are usually closed at both ends by fullerene-like halfspheres that contain both pentagons and hexagons [3]. Fig. 2(a) shows a SWNT with a well-defined spherical tip. A MWNT is represented in Fig. 2(b): the shape of the cap is more polyhedral than spherical. An open MWNT where the ends of the graphene layers and the internal cavity of the tube are exposed can be seen in Fig. 2(c).

Defects in the hexagonal lattice are usually present in the form of pentagons and heptagons. Pentagons produce a positive curvature of the graphene layer and are mostly found at the cap as in Fig. 2(b) where each knick in the graphene layers points to the presence of pentagons in the carbon network. Heptagons give rise to a negative curvature of the tube wall [34]. Defects consisting of several pentagons and/or heptagons have also been observed. A simple model indicates that the diameter and/or chirality of the tube is changed from one side of the defect to the other [35]. Such an arrangement forms therefore a link between two different tubes and is accordingly called a junction.

The electronic properties of SWNTs have been studied in a large number of theoretical works (see for example Refs. [2,3,36–38]). All models show that the

electronic properties vary in a predictable way from metallic to semiconducting with diameter and chirality [2,3]. This is due to the very peculiar band structure of graphene and is absent in systems that can be described with usual free electron theory. Graphene is a zero-gap semiconductor with the energy bands of the π-electrons crossing the Fermi level at the edges of the Brillouin zone, leading to a Fermi surface made of six points [39]. Graphene should show a metallic behavior at room temperature since electrons can easily cross from the valence to the conduction band. However, it behaves as a semi-metal because the electronic density at the Fermi level is quite low (about three orders of magnitude less than in metals) [29,39]. Rolling up the graphene sheet into a cylinder imposes periodic boundary conditions along the circumference and only a limited number of wave vectors are allowed in the direction perpendicular to the tube axis. When such wave vectors cross the edge of the Brillouin zone, and thus the Fermi surface, the nanotube is metallic. This is the case for all armchair tubes and for one out of three zig-zag and chiral tubes. Otherwise, the band structure of the nanotube shows a gap leading to semiconducting behavior, with a band gap that scales approximately with the inverse of the tube radius. Band gaps of 0.4–1 eV can be expected for SWNTs (corresponding to diameters between 0.6 and 1.6 nm) [2,3,37]. This simple model does not take into account the curvature of the tube which induces hybridization effects for very small tubes [36] and generates a small band gap for most metallic tubes [38]. The exceptions are armchair tubes that remain metallic due to their high symmetry.

These theoretical predictions made in 1992 were confirmed only in 1998 by scanning tunneling spectroscopy [4,5]. The scanning tunneling microscope has since then been used to image the atomic structure of SWNTs [40,41], the electron wave function [42] and to characterize the band structure [41,43]. Numerous conductivity experiments on SWNTs and MWNTs yielded additional information [14,15,44–53]. At low temperatures, SWNTs behave as coherent quantum wires where the conduction occurs through discrete electron states over large distances. Transport measurements revealed that metallic SWNTs show extremely long coherence lengths [45,53,54]. MWNTs show also these effects in spite of their larger diameter and multiple shells [55,56]. One striking example has been the observation of the Aharonov–Bohm effect [48,50].

Finally, pentagon–heptagon junctions have attracted a lot of attention. Joining a semiconducting to a metallic object on the scale of a few Å produces a semiconductor–metal junction on the atomic scale. The properties of such junctions predicted by several works [35,57–59] could be shown only a few months ago [60]: a metal–semiconductor junction behaves indeed like a rectifying diode.

The electronic properties and their dependence on the structure of the tubes are now well understood. There is, however, little information available on the impact of these two parameters on the field emission. A further concern is the electrical contact between the nanotube and its support: several articles have shown the difficulty of contacting reliably a nanotube to an electrode with a low ohmic resistivity [61,62]. We will come back to this point in the next sections.

3. Fabrication of carbon nanotube electron field emitters

A challenging part of many experiments is the growth of carbon nanotubes. At present there is no possibility to control the structure of nanotubes and all fabrication methods yield mixtures of nanotubes with different lengths, helicities and diameters. In addition, nanotubes can be further modified during post-growth treatments such as purification or annealing. In a first part, we will review the techniques used for synthesis and possible treatments. The focus of the second part will be the realization of carbon nanotube emitters.

3.1. Carbon nanotube synthesis

3.1.1. Arc discharge and laser ablation

The arc discharge was the first available method for the production of both MWNTs [1,63] and SWNTs [64,65]. It is worth noting that this technique has been in use for a long time for the production of carbon fibers and that it is very probable that nanotubes were observed before 1991 but not recognized as such [66,67].

MWNTs can be produced in a carbon arc apparatus similar to the one depicted in Fig. 3(a) using the method described by Ebbesen and Ajayan [63]. An arc is struck between two graphite electrodes in a gas atmosphere (usually He, but H_2 [68] and Ar have also been used) with typical values for the deposition bias and current of $U = 16$ V and $I = 80$ A at 400 mbar pressure. MWNTs produced by arc discharge are long and straight tubes closed at both ends with graphitic walls running parallel to the tube axis, as shown in Fig. 3(a).

Iijima et al. [64] and Bethune et al. [65] reported in 1993 that an arc discharge with a cathode containing metal catalysts (such as cobalt, iron or nickel) mixed to graphite powder results in a deposit containing SWNTs. The yield of the method has been significantly increased by optimizing the catalyst mixture [69] and the deposition conditions [70]. SWNTs are usually assembled in ropes as shown in Fig. 3(b) but some single tubes can also be found in the deposits.

Another method to grow SWNTs using laser ablation was demonstrated in 1996 [71] and has prompted a lot of interest. Thess et al. showed that the synthesis could be carried out in a horizontal flow tube under a

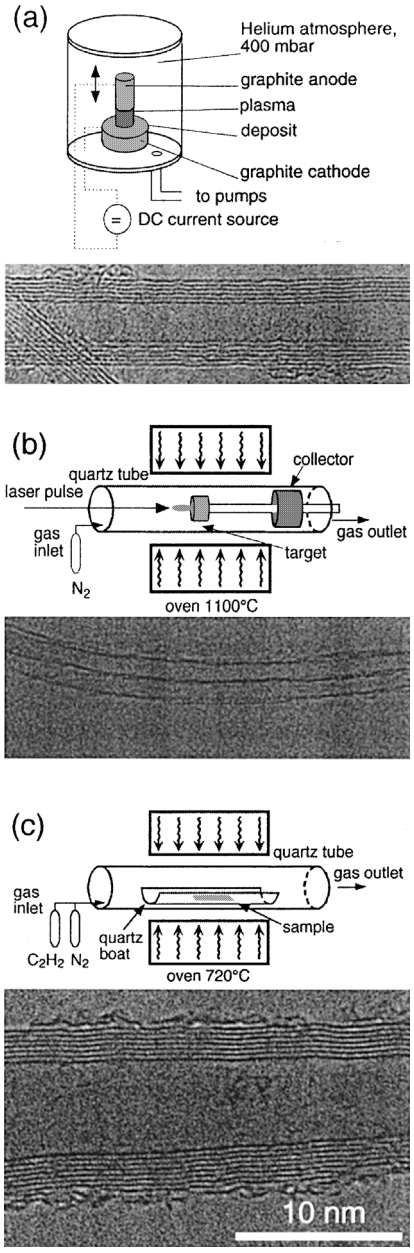

Fig. 3. Schematics of the different production techniques and corresponding TEM micrographs of the grown carbon nanotubes: (a) arc discharge, (b) laser ablation, (c) catalytic deposition. The micrographs are reproduced at the same magnification.

flow of inert gas at controlled pressure. In this setup the flow tube is heated to ~1100°C by a tube furnace as displayed in Fig. 3(b). Laser pulses enter the tube and strike a target consisting of a mixture of graphite and a metal catalyst such as Co or Ni. SWNTs condense from the laser vaporization plume and are deposited on a collector outside the furnace zone [72].

3.1.2. Catalytic growth

An alternative to the arc discharge and laser ablation methods is the catalytic growth of nanotubes. This method is based on the decomposition of a hydrocarbon gas over a transition metal to grow nanotubes in a chemical vapor deposition (CVD) reactor, as in Fig. 3(c).

Carbon filaments and fibers have been produced by thermal decomposition of hydrocarbons since the 1960s [73] (see also Ref. [74] for an overview). Usually, a catalyst is necessary to promote the growth [75]. Such fibers are either amorphous in nature, and must subsequently be graphitized by heat treatment [76], or are partly graphitized in a herring bone pattern [77].

A similar approach was used for the first time in 1993 to grow MWNTs from the decomposition of acetylene over iron particles [78]. A tube produced by catalytic growth is shown in Fig. 3(c). In general, the catalytic growth yields nanotubes of larger diameter as compared to the arc discharge, along with a crystalline structure that is not perfectly graphitized. [1] This may lead to problems as such defects were recently identified to be the areas of nanotubes that are most prone to electrical failure [79]. Finally, the ends of the tubes are mostly open, which according to some authors is a drawback over closed ends [80] and according to others an advantage [23,81].

For the production of MWNTs acetylene is usually used as source of carbon atoms at temperatures typically between 600–800°C. To grow SWNTs the temperature has to be significantly higher (900–1200°C) due to the fact that they have a higher energy of formation. In this case carbon monoxide or methane must be used because of their increased stability at higher temperatures as compared to acetylene. [2]

The catalytic method has undergone dramatic improvements in the last few years. Some rare SWNTs, along with MWNTs, were produced from a mixture of benzene and hydrogen at 1100°C [82]. Co catalysts supported on silica particles produced straight as well as coiled MWNTs [83], and the yield of nanotubes was significantly increased by using zeolites as catalyst supports [84,85]. Yield and average diameter of SWNTs were varied by controlling the process parameters [86]. In addition, the type of catalyst support was found to control the formation of individual or bundled SWNTs

[1] The distinction between nanotube and fiber is somewhat arbitrary. Usually the term nanotube is used if the walls are well graphitized and approximately parallel to the axis, with a diameter smaller than ~50 nm.

[2] At the temperature required for the production of SWNTs acetylene is unstable. This leads to the deposition of large amounts of other carbon modifications and only a limited amount of nanotubes is formed.

[87]. Recently, a technique for the continuous production of SWNTs, where both the carbon and the catalyst are supplied in the gas phase, was reported [86].

The catalytic method is also ideally suited to grow films of nanotubes on planar substrates such as silicon or glass. Dense MWNT arrays were thus deposited on mesoporous silica that was prepared by a sol–gel process [88] and aligned carbon nanotubes of more than 2 mm length were obtained over several square millimeters by using large-area mesoporous silica substrates [89]. Aligned MWNTs were generated by pyrolysis of a triazine compound at 950°C with nearly no by-products [90]. Nanotubes were also deposited by plasma-assisted CVD of methane and hydrogen at 950°C [91], and the synthesis temperature could be decreased below 660°C by using plasma-enhanced hot filament CVD [92]. Since then, several papers describing the synthesis of films of nanotubes on silicon substrates have been published [93–96]. Recently, microwave plasma-enhanced CVD of methane and hydrogen allowed to lower further the deposition temperature below 600°C on Ni-coated silicon [97], nickel [98], steel and Ni-coated glass [99] substrates.

A related technique is based on template growth [100]. The template, usually consisting of highly ordered alumina channels, is used to electrodeposit Co (or other catalysts) in the channels. Since diameters, density and length of the pores can be varied [100], large arrays of parallel carbon nanotubes with high periodicity and uniformity can be produced [100,101]. Unfortunately the structural quality is at present not as good as for nanotubes produced with alternative CVD methods.

There are several reasons behind the development of catalytic techniques to grow carbon nanotubes on planar substrates. In many cases, there are no or very few codeposited carbon allotropes. Cumbersome purification steps are thus unnecessary. Substrates can be directly patterned with catalysts using lithographic techniques followed by catalytic growth, as will be discussed in Section 3.2.4.

3.1.3. Purification

Most production methods yield a significant amount of by-products, which make purification mandatory. A first possibility involves chemical oxidation of the produced material in air or acid and damages in general the purified nanotubes. The second approach is based on physical separation and is typically done by filtration or chromatography of colloidal suspensions of nanotubes. Frequently, a combination of both methods is used.

Depending on the growth method, amorphous carbon deposited on the tube walls, nanoparticles consisting of nested closed graphitic layers of polyhedral shape, encapsulated transition metal particles and large graphitic fragments (>1 μm) are found as by-products. The latter contaminants can be easily removed due to their relatively high weight, for example by dispersing the powder in a solvent and subsequent centrifugation. The smaller particles are more problematic to eliminate. One possibility for MWNTs is to perform an oxidative treatment, either by heating the powder in air at 650°C [102] or by a liquid phase treatment in acidic environment [103,104]. The basal planes of graphite are subject to oxidation only if defects are present and small particles, which incorporate defects and/or reactive five-membered carbon rings, will therefore be preferentially attacked [105]. Unfortunately, the tube caps get invariably opened or at least damaged during the purification process [106]. For SWNTs, standard methods to eliminate catalyst particles and amorphous carbon involve refluxing the raw material in acid [107] followed by centrifugation or cross-flow filtration [72].

Another possibility for purification is to employ physical methods that do not damage the tubes but separate the objects as a function of their size. For MWNTs, a purification method which uses the properties of colloidal suspensions has been developed [108]. A sufficiently high concentration of surfactant is added to a water/raw product suspension. Smaller objects remain dispersed while larger particles form aggregates that sediment after a few hours. Residues with a nanotube content over 90% in weight were obtained as compared to 40% for the starting material. A related method, size-exclusion chromatography, was successfully used for the purification and size selection for MWNTs [109]. Purification procedures for SWNTs without any acidic treatment have also been reported and involve microfiltration [110] or size-exclusion chromatography [111].

3.2. Fabrication of carbon nanotube electron field emitters

Carbon nanotubes can be used as electron sources in two different types of setups, namely single and multiple electron beam devices. One possible application of a single electron beam instrument is an electron microscope that uses a single nanotube as a field emission electron gun to produce a highly coherent electron beam. Conversely, flat panel displays are the most popular example of multiple beam instruments where a continuous or patterned film of nanotubes provides a large number of independent electron beams. We present here the different methods that have been demonstrated for the realization of nanotube field emitters and discuss the different approaches to fabricate patterned films of nanotubes.

3.2.1. Single nanotube emitters

A field emission source with a single MWNT is easily realized. Electrochemically etched wires (e.g. W [112], Au [113], carbon fibers [23]) are usually used as support materials and in some cases spot welded on a wire loop for resistive heating. Individual nanotubes are then

mounted on the tips under an optical microscope equipped with two three-axes micromanipulators that are used to move independently the support and some nanotube material attached to the edge of a folded piece of conductive carbon tape [23,112]. Individual carbon nanotubes stick to the tip either by van der Waals forces alone [113] or by first applying a bit of conductive adhesive to the tip [112]. The resolution of an optical microscope is not sufficient to observe one nanotube and it is therefore highly recommended to systematically characterize the emitters by scanning [113] or transmission [112] electron microscopy. It is worth noting that emitters have also been realized by mounting the nanotube under a low-energy electron microscope equipped with micromanipulators [114].

The fabrication of the same type of device with SWNTs is more demanding since it is difficult to isolate a single tube from ropes and catalytic particles that are present in unpurified material. In that case, a macroscopic fragment of raw material is picked up with tweezers and is fixed on top of a tungsten tip [115]. The emitters are then made of many nanotubes. The interpretation of the results is not too problematic because the current of electrons emitted from a single nanotube can be measured using a probe hole in the counterelectrode (usually a phosphor screen). Another, more controlled technique involves attaching a SWNT rope to the support by careful approach of the tip to a mat of SWNT material under an optical microscope [116]. As soon as electrical contact is registered a small voltage ($\sim$10 V) is applied between the support and the SWNT mat to break the attached rope from the mat. Again, examination of the sample by scanning electron microscopy (SEM) or transmission electron microscopy (TEM) is mandatory. Other researchers used commercially available purified material where the tubes are segmented and well separated in the solution following an oxydation treatment [117]. This allowed to mount tubes with very little contaminating material. In that case however, the effect of the purification on the morphology of the tubes is not known (cap removal, presence of functional groups) and may affect the measured emission properties.

Another enticing method takes part of a manipulation tool that operates inside a scanning electron microscope [11]. Individual nanotubes can be picked up and attached to AFM cantilevers by electron beam irradiation, i.e., by dissociating residual organic species with the electron beam that are deposited onto the sample surface. These deposits are mechanically strong [11] and the electrical contact between the tube and the support should be strongly enhanced by the electron-beam irradiation [61].

Finally, the direct growth of one nanotube on a support by CVD is very promising. For example, AFM probes tipped with one single nanotube tip extending from the cantilever pyramid have been produced [17,18,20]. This opens up fascinating avenues for the characterization and application of nanotubes.

3.2.2. Continuous film emitters

A considerable research and development effort has taken place in the field of film emitters during the last decade. Historically, the first film emitters were realized by Spindt and coworkers by depositing Mo cones on grooved Si substrates to produce emitter arrays [118]. Commercial flat displays based on "Spindt"-type emitters are now available. The fabrication of such cathodes involves several processing steps and the cathodes themselves are quite sensitive to the ambient conditions. Alternative materials have thus been actively considered, in particular films based on carbon materials like diamond or tetrahedral-amorphous carbon.

De Heer et al. produced the nanotube film emitter presented in their seminal 1995 article [24] by drawing a colloidal suspension of MWNTs through a nanopore alumina filter. This film was then transferred by pressing the filter face-down on a teflon or teflon-coated metal surface [119]. This simple and fast preparation method can be used for all types of nanotubes [80,120]. Spraying the suspension on a heated substrate yields similar results [121].

Alternative film preparation techniques involve dispersing the tubes in a matrix. First experiments with colloidal graphite were described in 1994 already but no field emission could be observed [122,123]. Collins and Zettl dispersed purified MWNTs into non-conducting epoxies [124]. They then prepared emitters of 50×50 μm^2 area by drying the epoxy-nanotube matrix under pressure with a polishing to ensure a reproducible and macroscopically flat surface. Saito et al. used a similar method where MWNT material is crushed and mixed with products to form a paste [125] that is then applied on the metallic cathode and cured [126].

3.2.3. Patterned films using post-deposition techniques

One important prerequisite to using carbon nanotubes as electron emitters in some microelectronic devices is to be able to apply them in patterns onto the substrates. This can be realized either by producing the nanotubes and subsequent patterning on the support or by growing the nanotubes directly on a support prepatterned with a catalyst.

Wang et al. realized the first nanotube display by mechanically pressing a nanotube/epoxy paste into channels etched in a glass substrate [127]. The surface of the cathode was polished to expose the microchannels after curing. More recently, a 4.5 in. display was demonstrated by Choi et al. using SWNTs [128,129]. The purified SWNTs were mixed with an organic mixture of nitrocellulose and the resulting paste was squeezed onto a metal-patterned sodalime glass through a metal mesh.

The emitter was subsequently heated in order to remove the organic binder.

Similar methods involve the deposition of carbon nanotubes from a solution. For example, a resist layer was patterned by e-beam lithography on a substrate [130] and a nanotube dispersion was subsequently applied to the substrate. The nanotubes were allowed to precipitate in the resist openings and a patterned film was obtained after lift-off. The controlled deposition of individual MWNTs [131] and SWNTs [132] onto chemically functionalized surfaces has also been recently demonstrated. Individual nanotubes could be positioned at specific locations and orientations by applying a nanotube suspension on self-assembled monolayer templates defined by lithography.

3.2.4. Patterned films using direct growth on catalyst patterns

An alternative to fabricate patterns of nanotubes is to prepattern the substrate with a catalyst and to grow nanotubes onto these by CVD. The key step is therefore to deposit the catalyst at predefined locations and we will outline the techniques that are currently in use (see also Fig. 4).

The first patterned growth was demonstrated by Terrones et al. [90]. A thin cobalt film (10–100 nm) was deposited on silica by ablating a Co target with a laser. The film was exposed to air and linear tracks were etched with single laser pulses using a cylindrical lens. The laser etching produced Co particles along the edges of the eroded tracks which catalyzed the growth of MWNTs extending from the sides of the track [133].

The second technique involves standard lithographic techniques, such as photolithography or e-beam lithography. Basically, a resist is coated on the substrate, exposed and developed, creating a pattern of resist on the surface as shown in Fig. 4(a). The resist pattern can be used as a mask to deposit the catalyst on the unprotected part of the substrate creating thereby a negative of the resist pattern [87]. Conversely, the resist pattern is used as a protection when the catalyst is evaporated on the surface prior to the patterning, and the unprotected catalyst is removed with an acid or by plasma etching [134]. The resist is then removed by a solvent.

A comparable method was developed by Ren et al. with the idea to grow only one nanotube on each catalyst island. Well-separated single carbon nanotubes were thus grown on Ni dots 150 nm in diameter. However, the structure of the tubes resembles more that of carbon fibers since the graphitic planes are aligned at a 30° angle with the tube axis [135]. The tubes are tapered, with diameters of 150 nm at the base and significant variations in the height (up to a factor 10) are observed.

Fan et al. deposited an Fe film through shadow masks by e-beam evaporation onto plain and porous silicon substrates to control the position of the

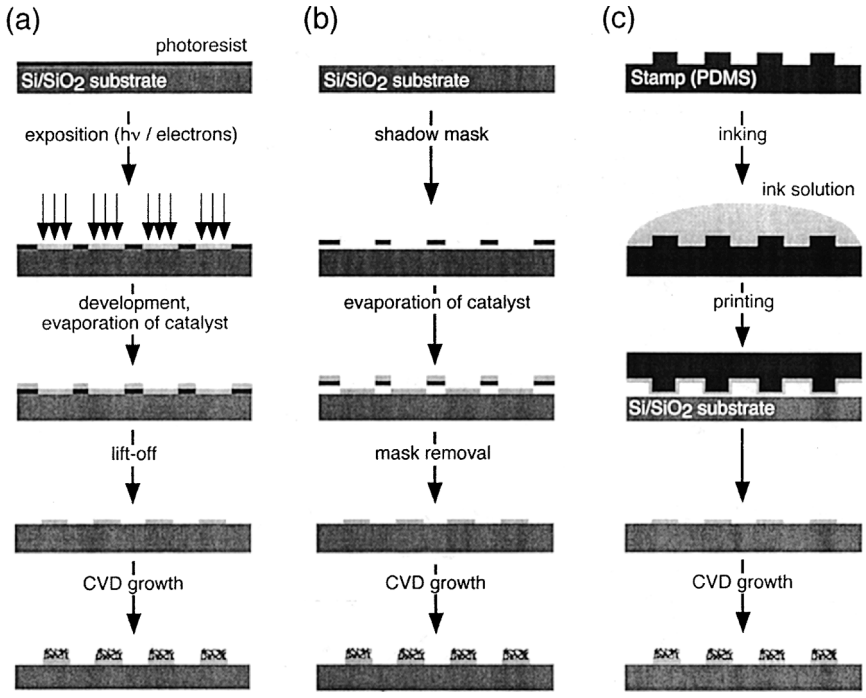

Fig. 4. Techniques to produce patterns of catalysts for the selective growth of carbon nanotubes: (a) standard lithography, (b) shadow-masking, (c) soft lithography.

nanotubes, as shown in Fig. 4(b) [93]. Nanotubes were then grown by acetylene decomposition at 700°C in flowing Ar. They were able to obtain three-dimensional arrays of nanotube blocks. Alternatively, arrays of vertically aligned carbon nanotubes were produced by CVD growth through shadow masks in contact with the substrate [136,137]. Masks were either photoresist patterns defined by lithography or physical objects like a TEM grid. The films could be transferred to other surfaces such as polymers that are unsuitable for CVD growth, and substrate-free films were obtained by immersing the quartz substrates into a HF solution.

Soft lithography, a non-photolithographic technique developed in 1993 by Whitesides [138], is another method to pattern surfaces with carbon nanotubes. The common feature of all variations of soft lithography is a patterned elastomer that permits a spatially controlled delivery of material to a surface using printing, molding, and embossing. Soft lithography is expected to be compatible with many liquid phase catalyst precursors for different catalyzed chemical reactions such as the catalytic growth of nanotubes [96,139]. In addition, the process is not based on the use of expensive equipment necessary to perform standard lithography.

For the patterned growth of nanotubes microcontact printing of catalyst precursors (μCP) can be implemented as schematized in Fig. 4(c). μCP uses a patterned and inked elastomeric stamp to transfer the catalyst precursor by mechanical contact to the substrate [96]. SWNTs or MWNTs can be grown on the pattern of catalyst depending on the combination of catalyst precursor, hydrocarbon gas and deposition temperature.

The stamps are made from poly(dimethyl)siloxane cured on masters prepared by photolithography. After peeling off the stamps from the master and hydrophilization in an O_2 plasma, the stamp surfaces are coated with the catalyst solution (called "ink"). Our ink of choice is an ethanolic solution containing 1–50 mM $Fe(NO_3)_3 \cdot 9H_2O$ aged for at least 12 h after preparation [140]. A conformal contact during printing is maintained for 3 s before the stamp is removed from the substrate. The deposition of nanotubes is carried out in a standard CVD flow reactor at 720°C as described earlier.

One of the main advantages of soft lithography is its compatibility with liquid catalysts. The choice of such a liquid catalyst allows one to vary its concentration over a large range and in turn to tune the density of nanotubes within the deposited film [140]. We demonstrate this additional control in Fig. 5. When the concentration is increased from 1 to 40 mM, we observe an increase of the density of the deposited nanotubes. For low concentrations (1 mM, Fig. 5(a)) only a few single nanotubes are distributed randomly over the printed zones. Increasing the concentration of the catalyst is accompanied by the formation of a film of entangled nanotubes as shown in Fig. 5(b) and (c) for 5 and 40 mM, respectively. Finally, a concentration around 50 mM results in arrays of nanotubes aligned perpendicular to

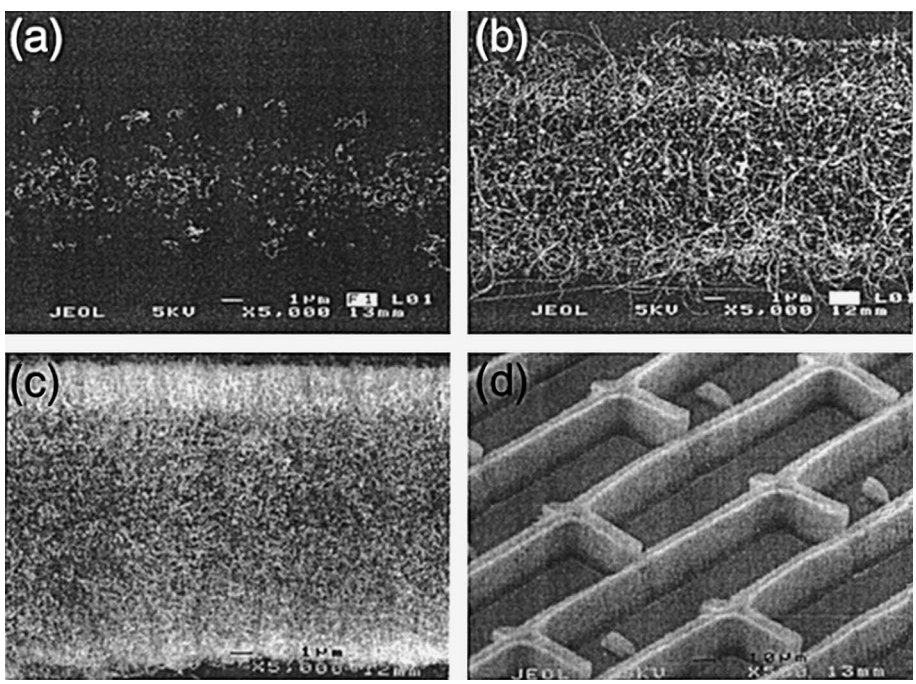

Fig. 5. SEM micrographs of patterned films of MWNTs prepared by μCP of a catalyst followed by CVD growth. The concentration of catalyst in the ink solution was (a) 1 mM, (b) 5 mM, (c) 40 mM, (d) 50 mM.

the surface similar to aligned assemblies of nanotubes found by other groups [90,92,93]. As displayed in Fig. 5(d), the side walls are flat and no tubes are branching away. High-magnification SEM images reveal that the top of the towers are smooth without nanotubes standing out at the top. For concentrations higher than 60 mM the growth of nanotubes is almost inhibited and the pattern is decorated by carbon particles.

A similar approach using μCP has been presented by Cassell et al. [141,142]. They used a flat stamp to transfer the catalyst onto a substrate consisting of regularly patterned silicon towers. Free standing SWNTs bridging the patterned towers could be formed by CVD of methane [143]. Finally, Huang et al. realized patterned films by forming carbon black structures to inhibit the growth of nanotubes [144]. The carbon black was realized by carbonizing a polymer pattern defined either by microcontact printing a self-assembling monolayer that prevented the adsorption of the polymer, or by molding the polymer with a structured elastomeric stamp. The nanotubes were grown in the polymer-free areas by pyrolysis of iron phthalocyanine and patterns with lateral dimensions down to 0.8 μm were demonstrated.

In summarizing these recent results, it becomes immediately apparent that all these lithographic methods show some advantages and disadvantages and it is difficult to figure out which of them will be the most suitable for the fabrication of gated devices. It is however important to note that most approaches use deposition temperatures that are too high. The necessity to grow the films at temperatures well below the melting point of glass (e.g. for flat panel displays) will be one of the main tasks in future.

4. Field emission from nanotube films

Let us first recall that field emission involves the extraction of electrons from a solid by tunneling through the surface potential barrier (for reviews on field emission see Refs. [145–149]). The emitted current depends directly on the local electric field at the emitting surface, E, and on its workfunction, ϕ, as shown in Fig. 6. In fact, a simple model (the Fowler–Nordheim model) shows that the dependence of the emitted current on the local electric field and the workfunction is exponential-like. As a consequence, a small variation of the shape or surrounding of the emitter (geometric field enhancement) and/or the chemical state of the surface has a strong impact on the emitted current.

These facts make a thorough comparison of results delicate, particularly because the methods used for synthesis (SWNTs, MWNTs), purification (closed or open ends, presence of contaminating material), and film deposition (alignment, spacing between the tubes) are quite varied. The interpretation is further complicated

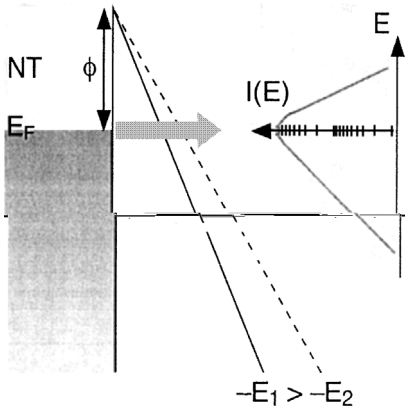

Fig. 6. Standard field emission model from a metallic emitter, showing the potential barrier and the corresponding FEED (energy on the vertical axis, current on the horizontal logarithmic axis).

by the different experimental setups, e.g., the use of planar, spherical or sharp tip anodes, and different interelectrode distances. Finally, the film surfaces used for emission are in some cases quite small (below 10^{-4} cm^2). With such dimensions, one nanotube emitting 10 μA is sufficient to yield an apparent current density of 0.1 A/cm^2. Sufficiently large emission surfaces (>1 mm^2) have to be considered to ensure that the measurement is representative. We will therefore distinguish between integrated (or macroscopic) and microscopic emission to explain the large variation of observed current densities from micron- to millimeter-sized areas.

4.1. Overview

We mentioned in Section 3 that nanotubes were produced and studied before Iijima identified them in 1991, and this applies probably also to field emission studies. In that respect, it is interesting to note that Chernotazonskii et al. reported field emission from "tubulene" films [22], i.e., from very dense MWNT films deposited on Si substrates [150] in 1995. The tube caps protruded only a few nm above the surface [151] and consequently the voltages needed to extract the current were very high [152]. De Heer et al. observed electron emission from a continuous film of randomly oriented arc discharge MWNT, with macroscopic current densities as high as 100 mA/cm^2 [24].

Most reports on the field emission describe the fabrication method of the film emitter and present a typical I–V curve. A short overview of results is given in Table 1 for each nanotube type, in chronological order.

Table 1 shows that field emission is excellent for nearly all types of nanotubes. The threshold fields are as low as 1 V/μm and turn-on fields around 5 V/μm are

Table 1
Emission characteristics of carbon nanotube films

Reference	Emitter	d (μm)	S (cm^{-2})	E_{to} (V/μm)	E_{thr} (V/μm)	J_{max} (A cm^{-2})	Remarks
[22]	MWNT	10–40	0.002	n.a.	<25*	1	Very dense "tubulene" film
[153]	MWNT	15	0.003	n.a.	~15*	10	Very dense "tubulene" film
[24]	Arc MWNT	20	0.008	n.a.	20*	0.1	
[154]	Arc MWNT	30	0.007	4.0	6.5		
[113]	Arc MWNT	125	0.07	2.6	4.6		
[79]	Arc MWNT	125	0.07	1.1	2.2		Purified sample with closed caps
[124]	Arc MWNT	20–100	2.5×10^{-5}	7.5*	10*	0.4	Open tubes dispersed in epoxy
[155]	Arc MWNT	80	0.025	0.9*	4*		O_2 plasma treated tubes dispersed in epoxy
[126]	Arc MWNT	200	0.02	n.a.	1.5		Tubes dispersed in epoxy
[120]	SWNT	125	0.07	1.5	3.9		
[156]	SWNT	10–300	0.002	n.a.	4–7	4	
[157]	SWNT	150	3.1	2.1*	n.a.		
[91]	CVD MWNT	n.a.	0.001	1.7*	n.a.		
[93]	CVD MWNT	70	n.a.	n.a.	4.8–6.1		Aligned MWNTs, 15 emitters
[158]	CVD MWNT	150	3.1	n.a.	2.1*		Large amount of graphitic fragments
[134]	CVD MWNT	n.a.	0.0003	4.8	6.5	0.1–1	
[159]	CVD MWNT	600	0.07	n.a.	$\geqslant 5$		
[160]	CVD MWNT	150	0.2	3	6.6*		Si substrate
[99]	CVD MWNT	500	0.1	1.6	5*		Steel substrate
[99]	CVD MWNT	500	0.1	3	5.6*		Ni substrate
[161]	CVD MWNT	10–300	0.002	0.75	1.6	1–3	Catalyst supplied in gas phase
[162]	Graphitic fibers	300	1–10	2.1	n.a.	0.2	

d is the interelectrode distance, S the emission area, E_{to} and E_{thr} are the turn-on and threshold fields needed to produce an integrated current density of 10 μA/cm^2 and 10 mA/cm^2, and J_{max} is the maximal current obtained without destruction of the emitter. n.a. means that the value is not indicated or could not be deduced from the figures, and * indicates that the value was estimated or extrapolated from the presented data.

typical. Nanotube films are capable of emitting current densities up to a few A/cm^2 at fields below 10 V/μm.

One interesting parameter is the actual emitter density on the films. Typically, a film has a nanotube density of 10^8–10^9 cm^{-2}. The effective number of emitting sites, however, is quite lower. Typical densities of 10^3–10^4 emitters/cm^2 were reported at the onset of emission [24,113,156,163]. By using an optical microscope combined with a phosphor screen, Obraztsov et al. were able to enhance the resolution of the measurement and reported densities of 10^7–10^8 cm^{-2} [160].

4.2. Comparison of different films under identical conditions

A more detailed study of Table 1 reveals that the type of tubes has no conclusive influence on the field emission properties. We address this point now in more detail by discussing results acquired on different nanotube films under the same experimental conditions. This will allow to shed more light on the influence of the different parameters on the field emission. Some important parameters are summarized in Table 2.

We can extract from Table 2 that several parameters have an impact on the emission. First, the intrinsic structural and chemical properties of the individual tubes play a role, as marked differences were found depending on the diameter [79] and surface treatment [164] as well as between closed and open tubes [79]. Second, the density and orientation of the tubes on the film [79,101,121] influences also the emission. The comparison and interpretation of the results is difficult because most groups either use different experimental procedures, vary several parameters or did not characterize completely their samples. It is hence unclear whether the observed variations in field emission properties are due to different intrinsic properties of the tubes (e.g., SWNTs as compared to MWNTs) or to the preparation method. To illustrate this, we observed a slightly inferior emission for SWNTs than for randomly aligned MWNTs

Table 2
Emission characteristics of carbon nanotube films studied under identical conditions

Reference	Influence	Emitter	d (μm)	S (cm^{-2})	E_{to} (V/μm)	E_{thr} (V/μm)	Remarks
[101]	Density and geometry	MWNT	25	n.a.	<2.7*	~4.8*	Random alignment
[101]		MWNT	25	n.a.	~40*	n.a.	Short vertical tubes
[79]	Geometry	Arc MWNT	125	0.07	2.6	4.6	Average over 15 emitters
[79]		SWNT	125	0.07	2.8	5.2	Average over 12 emitters
[79]		Open MWNT	125	0.07	4.5	30	Average over six emitters
[79]		Graphitic fibers	125	0.07	5.6	14	Average over five emitters
[164]	Surface treatment	MWNT ta-c coated	125–400	0.01	1.6	n.a.	
[164]		MWNT (as produced)	125–400	0.01	2.4	n.a.	
[121]	Density and geometry	SWNT	10–500	10^{-5}	n.a.	2.4	Randomly aligned
[121]		CVD MWNT	10–500	10^{-5}	n.a.	3.5	Dense aligned arrays
[165]	Density	CVD MWNT	125	0.007	9.8	14.4	Low density, patterned films (Fig. 5(a))
[165]		CVD MWNT	125	0.007	2.2	3.3	Medium density, patterned films (Fig. 5(b))
[165]		CVD MWNT	125	0.007	3.6	5.3	High density, patterned films (Fig. 5(c))

The symbols are the same as in Table 1.

[79] while Bower et al. measured the inverse behavior for SWNTs and densely aligned MWNTs [121]. We address this problem in Section 4.3 where only the density of nanotubes on the film was varied.

4.3. Comparison between nanotube films of different densities

We will now discuss the influence of the density on the macroscopic field emission obtained from patterned samples fabricated and measured under identical conditions [165]. A careful study of the patterns revealed that the density and length of the tubes were the only two parameters which changed from sample to sample. Fig. 5(a)–(c) shows SEM micrographs of three representative samples. The corresponding I–V curves are given in Fig. 7, while the turn-on and threshold fields can be found in Table 2.

Our best emitter corresponds to the film shown in Fig. 5(b), followed by the film in Fig. 5(c). The worst emitter is the film of Fig. 5(a). The analysis of eleven samples of different densities proved that films of medium densities with nanotubes protruding over the film surface show emission at the lowest fields [165].

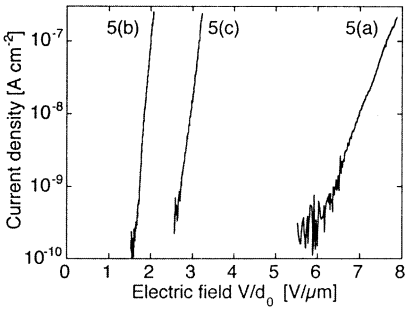

Fig. 7. Field emission I–V curves of MWNT films of different densities. The left, middle, and right characteristics were acquired on the films of Fig. 5(b), (c), and (a), respectively.

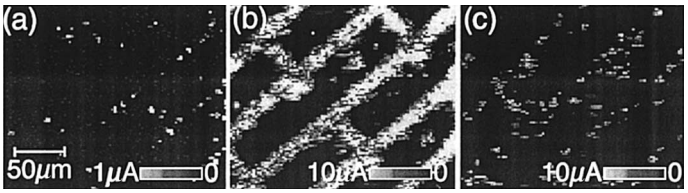

Fig. 8. Scanning field emission images of MWNT films of different densities acquired at constant voltage and tip height. The greyscale represents the current intensity. Images (a)–(c) were taken on films similar to those of Fig. 5(a)–(c), respectively.

Further clues can be gained by characterizing the emission on a microscopic scale. A vacuum FE apparatus was used to locally resolve field emission using a scanning tip [166]. The scanned area was typically 200×200 μm^2 with a Pt–Ir anode of 2–5 μm tip radius biased to ~100 V. The separation between anode and the surface of the emitting film was fixed at ~3–5 μm. Fig. 8 depicts the results of three emission scans on patterned samples of different densities and similar to the ones shown in Fig. 5(a)–(c) [166]. The low density sample shows a rather inhomogeneous emission pattern with very few sites emitting a low current (Fig. 8(a)). A much more homogenous emission image is obtained for a medium density (Fig. 8(b)). The lines, bridges and dots of the structured film can be easily distinguished. Finally, a sample of high nanotube density yields a result similar to the low density one, albeit with an emission intensity higher by a factor of 10 (Fig. 8(c)).

These results complement the macroscopic characterization. We may readily understand that a film of low density and short tubes will be an inefficient cathode. The medium density films show a very homogeneous and strong emission with a large number of emitting sites. A very dense film, however, shows a decreased quality of the emission. This results from a combination of two effects: the intertube distance and the number of emitters. When the intertube distance is large, the field amplification factor is determined only by the diameter and the height of the nanotube. As the distance between the tubes is decreased, screening effects become significant. [3] Since the number of emitters increases with decreasing intertube distance, there will be an optimum distance for a maximal emitted current density. The calculations indicate that this distance amounts to 1–2 times the tube height [166]. The height of the tubes over the substrate (or the average film surface) is of course another important parameter [166]. In fact, the influence from the substrate – or from the average film surface – is significant even for long tubes.

[3] In fact, electrostatic calculations show that the field amplification factor decreases already when the intertube distance amounts to twice the height of the tubes and drops rapidly for smaller distances.

Our three samples correspond therefore to three different emission regimes. The turn-on fields for low density films are high because there are few emitters with short heights. Conversely, the emission from high density films is more efficient but remains low because of screening effects between densely packed neighboring tubes and because of the small height of the tubes. There is an ideal compromise between these two extremes, where the length of the tubes and the distance between neighboring emitters are both sufficient to reach a high field amplification along with an emitter density that is high enough to ensure homogeneous emission at low voltages.

4.4. Degradation of nanotube films

For any future application, the prerequisite of the long-term stability of the emitting films must be fulfilled. The degradation of the emission is usually due to several phenomena and can be either reversible or permanent. Irreversible damage can occur through resistive heating, bombardment from gas molecules ionized by the emitted electrons, or arcing. Electrostatic deflection or mechanical stresses can cause alterations in the shape and/or surroundings of the emitter and lead to a decrease of the local field amplification. Other degradation phenomena are of chemical origin (adsorption or desorption of molecules on the emitter surface) and modify the workfunction.

A stable emission over more than 20 h was observed by several groups on MWNT films for current densities of ~1 mA/cm^2 [24,93,159,162]. The longest test up-to-date has been performed by Saito et al. who report an increase of 11% of the applied field to maintain an emission current of 10 mA/cm^2 during 8000 h [126].

Other studies show nevertheless that degradation can occur on shorter time scales. At present the origin of degradation is not clear. It seems that residual gases have a significant influence [113,128] and that the emitted current density is important as well [79,156]. In addition, the intrinsic properties of nanotubes also have an importance. A comparison between films of SWNTs and MWNTs at comparable chamber pressure (10^{-7} mbar) and emitted current density (0.2 mA/cm^2) showed that the degradation was a factor of 10 faster for SWNTs

[79,120]. The faster degradation of SWNTs was attributed to the fact that their single shell makes them more sensitive to ion bombardment and irradiation, while the multiple shells of MWNTs tend to stabilize their structure.

Adhesion problems of patterned films under high applied fields were reported by Nilsson et al. [167]. It could thus be that very dense films, like those of Fig. 5(d), have a better long-term stability due to the high mutual entanglement than films with lower density where the nanotubes may more easily be deflected [168], irreversibly bent or even detached by the applied field.

Finally, the configuration used for emission (parallel plates or plan-to-sphere configurations with distances of ~100 μm, or field emission microscope setups with far larger interelectrode distances) may also play a role. Dean et al. suggested that the poor vacuum conductance between two closely placed planes leads to high local pressures of gases like water or oxygen that cause reactive etching and hence faster degradation (see also Section 5.4) [117].

5. Field emission from single nanotubes

This section reviews the experiments carried out on single nanotube emitters, which give us a reliable way to obtain information on the emission mechanism and the workfunction.

The first electron field emission from a single nanotube was reported by Rinzler et al. who studied an arc-produced MWNT mounted on a carbon fiber [23]. A complementary paper showed that the emission followed roughly a Fowler–Nordheim behavior and currents of ~100 nA were drawn at 0.12 V/μm [169].

We studied closed and open arc discharge MWNT nanotubes mounted on gold fibers as shown in Fig. 9 [79,113]. The emission at low currents followed a Fowler–Nordheim behavior up to currents of 5–20 nA for closed and open tubes (Fig. 9). As the current was further increased small slope changes and sometimes strong saturation effects were observed. We noted that all emitters were capable of emitting over an incredible current range: currents up to 0.1 mA per tube were reached repeatedly on all emitters and a maximal current of 0.2 mA was drawn from one tube [113]. Finally it was found that open tubes emitted at about twice the voltage needed for the closed ones, as is shown in Fig. 9 [79].

In contradiction to our results, Saito et al. found that open MWNTs began to emit electrons at the lowest fields, followed by MWNTs produced in hydrogen and finally closed arc discharge MWNTs [80,115,126]. The observed differences are probably due to the fact that they used other methods to grow and mount the nanotubes which resulted in variations of sample purity and emitter geometry.

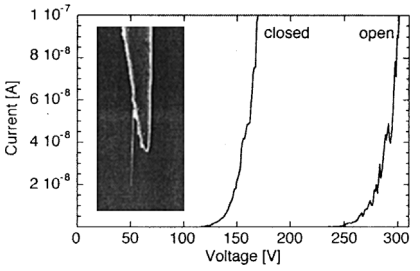

Fig. 9. Field emission I–V curves acquired on a single closed and open MWNT mounted on the apex of an etched gold fiber of 20 μm diameter as shown in the inset.

5.1. Emitter stability and failure

One point noted by nearly all researchers is that the I–V characteristics of nanotubes does not follow a Fowler–Nordheim behavior over the whole current range. This is apparent for both films [113,164,170] and single emitters.

This peculiarity can be accompanied by changes in the emission stability for SWNT films and for MWNTs [79,113]. Two different current regimes were observed: step-like fluctuations at low emitted currents with a switching frequency that increased with the current and became maximal at the onset of saturation, followed at higher currents by stable emission with flicker noise. Similar current fluctuations at low currents were observed by Saito et al. [126]. We attributed the observed saturation to the presence of non-metallic resonant states at the cap (see also below).

Dean et al. observed the same saturation phenomena on single SWNTs [171]. The onset of saturation occurred for currents of 0.1–0.3 μA and was accompanied by increased current fluctuations. These fluctuations disappeared nearly completely at higher currents. This behavior was ascribed to the presence of adsorbates (most probably water) at the cap that enhance the field emission as compared to clean caps. Field emission microscopy (FEM) (see also Section 5.2) showed typical adsorbate patterns that were stable at low currents but changed shapes at the onset of saturation. An adsorbate-free pattern was detected as the current increased beyond the saturation. The interpretation of Dean et al. is that the emission occurs through the adsorbate at low voltages on a pristine tube. The saturation results from the displacement of the adsorbates, followed by their desorption as the voltage is further increased.

We expand hereafter the discussion of Section 4.4 on the emitter lifetime and consider single emitters. In contrast to films where the degradation is gradual, the decline of a single nanotube is in nearly all cases abrupt. For single closed MWNT stable emission was observed at 2 μA for more than 90 h at 10^{-7} mbar [113]. Typical behavior of metallic cold field emitters, i.e., a gradual

and reversible decrease due to the formation of absorbed layers, was not observed. Termination of the emission happened on most emitters as a catastrophic and irreversible failure that occurred in less than 10 ms. Fransen et al. measured one MWNT during more than two months at 0.4 μA at 10^{-9} mbar without any observable degradation [112].

To assess the influence of the gas environment on the emission stability, Dean et al. measured the emission of SWNTs under different gas exposure [117]. No degradation was measured on a single nanotube over more than 350 h with an emitted current of 3 μA at 10^{-9} mbar. Conversely, irreversible continuous decreases in the current were provoked by exposure to oxygen and water and were attributed to reactive sputter etching. In contrast, exposure to Ar and H_2 did not lead to permanent damage.

The mechanism that leads to the catastrophic failure of a single nanotube is not completely understood, but some interesting hints are already available. De Heer et al. presented recently some experiments of field emission on single MWNTs in a transmission electron microscope [172,173]. It appears that tube failure occurs on a very short time scale (<1 ms) at currents above 0.1 mA and that it involves an irreversible damage to the tube. Tube layers or caps are removed, peeled back, or the end of the tube is amorphized [173]. In all cases a strong decrease in the emission current occurs and the voltage has to be substantially increased to obtain comparable currents. Cumings and Zettl observed single MWNTs with a similar setup [174]. They were able to "peel" the tube layer by layer by applying a strong current through the tube. De Pablo et al. proved that the location of the electrical failure on a single MWNT could be correlated with the presence of a defect in the nanotube [79].

We see that the understanding of emitter degradation is yet fragmentary. Single nanotubes are stable emitters in UHV, whereas film emitters show in some cases a gradual decrease of the emitted current. It is at present not clear if the degradation of one tube in a film is abrupt or gradual.

5.2. Field emission and field ion microscopy

FEM has been extensively used in the past 60 years in surface science [145,146,149]. In such an experiment a phosphor screen is used as the counterelectrode and the obtained pattern reflects the spatial distribution of the emitted current. Since the emitted current depends critically on the local field amplification and the workfunction, FEM has been used with great success for diffusion and adsorption/desorption studies as well as to determine the workfunction from different surfaces (see Section 5.3). FEM is often used in combination with field ion microscopy (FIM), which can be performed with the same setup but with a positive applied voltage under partial pressure of an imaging gas (He or Ne) [145,146,149]. The gas atoms are ionized by the high local electric field at surface steps and salient atoms, accelerated by the potential difference and impact on the phosphor screen. FEM and FIM are of great interest since they offer a direct way of visualizing the spatial distribution of the emitted electrons as well as the atomic structure of the cap. These expectations have not quite been fulfilled yet for nanotubes, even though several groups performed such experiments with sometimes contradictory findings.

Saito et al. obtained FEM patterns from closed MWNTs and observed single bright spots with dimensions that suggested that the emission proceeds from the whole cap of MWNTs and not from a few atoms only [115]. Ring patterns with a dark center were detected on open MWNTs and were interpreted as originating from the edges of the graphene layers of the open MWNT [175]. SWNTs patterns were similar to those of closed MWNTs and were assigned to SWNT ropes [176].

We also detected bright spots from MWNT and SWNT emitters along with well-defined patterns of two or fourfold symmetry [79,177]. These patterns persisted after applying high positive fields to desorb eventual adsorbates and reflect probably the electronic density of the emitting states at the nanotube cap. The non-homogenous density would identify them as localized states at the cap and not as delocalized conduction-band states as in metals.

On purified SWNT films, Zhu et al. found ring patterns that were interpreted as coming from nanotube ends because of the circular symmetry [156]. Ma et al. observed circular arcs and rings on films of open-ended fibers that were attributed to emission from the open edges [162].

Dean et al. measured FEM on SWNTs at room temperature as well as at 600°C [178]. At room temperature, the patterns show one to four lobes that are typical of, and behaved like, molecules adsorbed on the tube cap. These patterns disappeared above 600°C, and fine-structured patterns with sometimes five or sixfold symmetry were detected. Dean et al. argue that these patterns represent the electronic distribution of the emitting states at the nanotube cap and not the atomic structure of the cap.

Lovall et al. tried to image the cap of a SWNT by FIM using He as the imaging gas [116]. The resulting pattern was composed of ring structures consisting of several features located around the circumference of the ring with two or three additional faint features located inside the innermost ring. The image is compatible with the edge atoms of an open SWNT, and the observed SWNT was tentatively identified as a tube of 28° chiral angle and 2.1 nm diameter.

In summary, some tubes produce homogenous spot or ring patterns that are quite similar to those observed on metal tips. On the other hand, the observation of fine-structured stable patterns strongly suggests that the electronic distribution of the emitting states is not homogenous. The origin of this discrepancy is not clear at present and could be due to experimental problems as well as to instrinsic differences between SWNTs, closed and open MWNTs. A highly desirable future study would be a combined FEM/FIM observation of nanotube caps: the repartition of the emitted current could be directly correlated to the atomic structure and thereby allow an unprecedented characterization of the electronic states at the nanotube cap.

5.3. Field emission energy distribution and workfunction

One aspect of field emission that has not been discussed yet is the influence of the electronic properties, more specifically of the electronic density of states (DOS), on the field emission. In metals, the DOS of the conduction electrons, which are responsible for the emission, is described by the Fermi–Dirac statistics. The workfunction, ϕ, corresponds to the energy difference between the Fermi level and the top of the surface barrier as shown in Fig. 6. Above the Fermi level the tunneling probability increases but the DOS decreases very sharply. Below the Fermi level the DOS increases slightly but the tunneling probability decreases strongly. These considerations are directly reflected in the specific shape for the field emission energy distribution (FEED) of the electrons predicted by the Fowler–Nordheim theory (see Fig. 6). The FEED peaks around the Fermi level with exponential tails that depend on the Fermi temperature of the electrons and on the slope of the tunneling barrier for the high and low energy tail, respectively [146–148]. Any deviation from this metallic shape is due either to adsorbates [147] or to a non-metallic DOS [179]. FEED can therefore be used to gain information on the DOS of the emitting electrons as well as to determine the workfunction.

The FWHM (full width at half maximum) of the FEED is typically 0.45 eV for a metal [147]. Measurements on nanotubes consistently show that the FEED is significantly narrower and additional features suggest that the emission is more complicated than for a metallic emitter. A measurement of the FEED was first attempted by De Heer et al., who reported a narrow peak of 0.21 eV on a MWNT film at the onset of emission [177]. Spectra consisting of several peaks were also observed. The fact that an assembly of tubes was used made the interpretation of these features difficult: the multiple peaks could arise either from one tube only (which would point to a non-metallic DOS) or from several tubes (having either different voltage drops across the tube or the contact, or non-metallic DOS located at different positions with respect to the Fermi level). The shape of the FEED suggested that the emission occurred from energy bands of 0.2–0.4 eV width (Fig. 10(a)) [80].

Fransen et al. observed two kinds of behavior on single MWNT emitters [112]. Some spectra showed one peak of ~0.3 eV FWHM that shifted with the applied field. These peak shifts were due either to a voltage drop in the contact area between the tube and the support or to field penetration in the tube. Other spectra were composed of several peaks of ~0.15 eV FWHM that did not shift with the voltage. The small FWHM was attributed to the presence of resonant states in the DOS at the tube cap.

Dean et al. detected one peak located at the Fermi level on a single SWNT at room temperature consistent with a metallic, localized or adsorbate state (Fig. 10(b)) at the Fermi level [180]. No peak shift was observed on

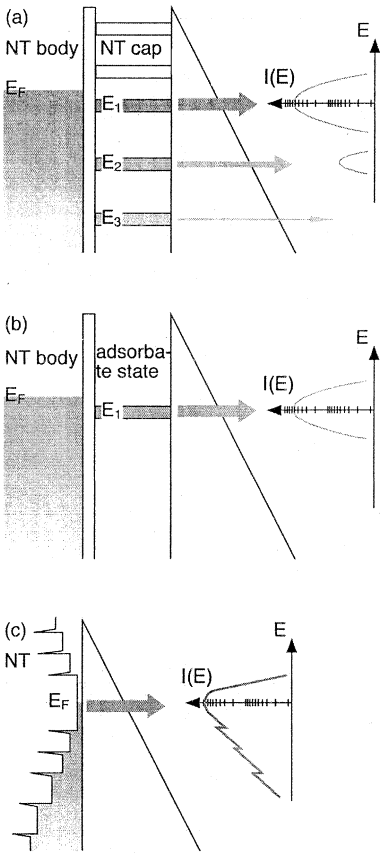

Fig. 10. Models for the field emission from nanotubes, showing the energy bands in the different part of the nanotube, the potential barrier, as well as the corresponding FEED (energy on the vertical axis, current on the horizontal logarithmic axis). (a) emission through energy bands corresponding to electronic states localized at the nanotube cap, (b) adsorbate resonant tunneling, (c) emission from a typical metallic SWNT DOS.

changing the applied field. A decrease in the emitted current along with an increase in the FEED signal occurred when the temperature was increased to 600°C and was attributed to adsorbate removal. A further increase in temperature resulted in the appearance of additional peaks in the spectrum above the Fermi level. Since the FEED is a convolution between the tunneling barrier and the electronic DOS of the nanotube, they concluded that tunneling states are present above the Fermi level in clean SWNTs (Fig. 10(a)).

Lovall et al. detected unusual features in the low energy tail of FEED spectra from one SWNT at room temperature [116]. Small shoulders located at 0.64 and 1.05 eV below the Fermi energy were attributed to singularities in the DOS of the SWNT (Fig. 10(c)) [3,4]. Although the diameter and chiral angle could not be univocally determined on the basis of the two features, the range of possible emitter structures could be significantly narrowed.

The narrow FWHM observed at room temperature is either due to the instrinsic electronic properties of the tube or to resonant tunneling through adsorbates, and future studies will hopefully clarify this point. It seems certain, however, that some features of the DOS of the tubes (or the tube caps, see Section 5.4), such as resonant localized states and/or singularities, are reflected in the FEED spectra.

Experimental results on the workfunction are fragmentary. Fransen et al. determined a workfunction of 7.3 ± 0.7 eV on one MWNT [112]. Küttel et al. found a workfunction in the 5 eV range for a CVD MWNT film [163] which was refined to 5.3 eV in a subsequent study [181]. Lovall et al. deduced a value of 5.1 eV for a single SWNT from the slope of the I–V curve, having beforehand characterized their emitter to assess reliably the field amplification factor. Very low values between 0.5 and 2 eV have also been reported for MWNT films from the slope of the Fowler–Nordheim plot [153,158]. The field amplification factors were determined from the average radius and height of the tubes using well-known formulas. This approach is possible, however, only in the case of a single emitter because there is a significant influence from both neighboring tubes and substrate on a film, as we have seen in Section 4.3. It seems far safer to make an assumption on the workfunction and to deduce the field amplification (and emitter shape [113]) than work the other way around. FEED remains the only reliable method to determine simultaneously the workfunction of a field emitter and the field amplification factor [163,181].

It is not clear so far if the workfunction of closed MWNTs, open MWNTs or SWNTs are different. The workfunction might even be different from one tube to the next. One can expect a variation in workfunction between the basal plane of graphite and its open edge, as shown by simulations [182]. The termination of the graphene layers of an open nanotube should also have a strong influence. A workfunction of 6.3 eV was predicted for a clean graphene edge, to be compared with workfunctions of 3.31 and 7.29 eV for a H- and a O-terminated edge, respectively [182].

Finally, ultraviolet photoelectron spectroscopy measurements performed on MWNT films gave a clear indication that the workfunction can vary significantly with the surface state of the tubes [183]. This underlines once again the uttermost importance of emitter preparation, and shows that the properties of the tubes may be significantly influenced by the synthesis and purification methods.

5.4. Field emission mechanism

Why are nanotubes such exceptional field emitters? The very low turn-on fields measured for nearly all emitters originate certainly from the small diameter and elongated shape of the tubes that lead to a high geometrical field enhancement. In fact, the local electric field just above the emitter surface needed for field emission is around 2–3 V/nm as for metallic emitters, as can be estimated from the applied field and the field amplification factor [91,113,165]. On the other hand, nanotubes do not behave like very sharp metallic tips. Furthermore, the influence of the structural properties of the tube on the field emission is not clearly assessed at present. This issue is complicated by the fact that the physical and chemical properties are deeply modified by preparation and purification steps [23,79,126,169]. Despite these difficulties we will summarize here the principal models that have been proposed for the field emission from carbon nanotubes.

Some authors recorded I–V characteristics that follow the Fowler–Nordheim law (at least over a certain current range), from which they concluded that carbon nanotubes behave as metallic emitters (Fig. 6) [115, 155,163].

Rinzler et al. interpreted the higher efficiency of open MWNTs and their behavior under laser irradiation as emission from a single carbon chain that unravels from the tube edge and produces a very high field amplification [23]. This model could not be confirmed yet experimentally, and would probably be valid only for open tubes.

Obraztsov et al. proposed that the graphene layers form sharp bends at the open end of the nanotube, where the carbon atoms show sp^3-like atomic bonds instead of the sp^2 configuration typical for graphene [157,158,160]. This change in coordination would decrease the height of the potential barrier and could explain the very low workfunction that the authors estimated from the slope of Fowler–Nordheim plots. Again, this model would be valid only for open MWNT.

We concluded from our observations that the electrons are emitted from sharp energy levels due to localized states at the tube cap as shown in Fig. 10(b) [79]. Luminescence induced by the electron emission could arise from radiative transitions between two levels participating to the field emission [184]. Actually, theoretical calculations predict the presence of localized states at the tube cap, with a DOS that differs markedly to that of the tube body [185–187]. This was recently confirmed experimentally by STM measurements on MWNTs [186] as well as on SWNTs [141]. The FWHM of these states and their separation is in good agreement with the values measured for the light emission and with FEED observations carried out at 20°C [112] and at 600°C [180].

Two points have to be mentioned concerning this hypothesis. If several energy levels participate in the emission, the occupied level nearest to the Fermi energy will supply nearly all the emitted electrons. Since the position of this level would depend strongly on the local atomic configuration (tube diameter, chirality, presence of pentagons and other defects), significant differences of the emitted currents can be expected from one tube to another. Second, these localized states often show far higher carrier densities as compared to the tube body at the Fermi level [186]. As the field emission current depends directly on this carrier density, we speculate that the emitted current would be far lower for a nanotube without such states.

A complete study by Dean et al. suggests complementary mechanisms, and shows clearly that the emission behavior of nanotubes is far more complex than the one expected from a very sharp metallic tip with a workfunction of $\sim$5 eV [171,188]. Different emission regimes on single SWNTs were identified and depended on applied field and temperature. A first regime corresponding to resonant tunneling through an adsorbate (Fig. 10(b)) was found under "usual" experimental conditions at low temperatures and applied fields. The involved molecule has been identified as water and it appears that this adsorbate-assisted tunneling is the stable field emission mode at room temperature. These molecules desorb either at high fields and emitted currents or at temperatures higher than 400°C. The other regimes correspond to the intrinsic emission from the cleaned tube and show a far lower emitted current for comparable voltages with strongly reduced current fluctuations. The origin of these (at least two) instrinsic regimes is not clear yet but the emission mechanism involves probably non-metallic electronic states, such as enhanced field emission states above the Fermi level or a non-metallic DOS.

In short, the present understanding is that the emission involves a non-metallic DOS and/or adsorbate-resonant tunneling. Supplementary informations on the electronic structure of the nanotube cap and on the influence of absorbates or bonded groups are required for a better comprehension of the emission. It seems us important to mention again the work of Lovall et al. [116]. They show the way for a complete characterization of nanotubes, where the electronic DOS is measured by FEED and the exact structure of the tube cap is determined by FIM. This simultaneous determination of the electronic and structural properties of individual nanotubes would without doubt yield valuable insights on the emission mechanism.

6. Field emission applications

Despite the demonstration that a single MWNT emits monochromatic electrons over long periods of time at low applied fields, we know of only one instance where a single nanotube has been used in a high-resolution electron beam instrument. Fink et al. developed a low energy electron projection microscope where the electrons are extracted by applying a voltage between the sample and a MWNT emitter [189]. The nanotube provided a highly coherent beam that allowed the acquisition of in-line electron holograms of the observed objects with a quality comparable to atom-sized W emitters [114].

It is not proven yet that single nanotubes can be used in other instruments such as scanning or transmission electron microscopes [190]. Nanotube emitters show higher coherence and narrower FEED than cold or Schottky cathodes used in such instruments and might provide an interesting alternative [112].

In contrast to single nanotube devices, applications based on an assembly of nanotubes are diverse. Nanotube flat-panel displays were proposed early on as an enticing alternative to other film emitters [22,24]. It took only three years until the first display with 32×32 matrix-addressable pixels in diode configuration was realized by Wang et al. [127].

Choi et al. recently demonstrated a fully sealed 4.5 in. three color field-emission display [128,129]. The display, reproduced in Fig. 11 has 128 addressable lines and works in diode configuration. Since then, the Samsung research group has shown a 4.5 in. device displaying full-color images [191] and later a 9 in. full-color display with 576×242 pixels [192].

As indicated in Section 3, there are numerous technological hurdles related to the deposition of nanotubes in gated structures. Problems such as display sealing, phosphor lifetime, and charging of spacers are further concerns. Other, simpler devices than flat-panel displays have been demonstrated up to now and there are probably many more under investigation.

One possibility is to use nanotubes in lighting elements, i.e., to produce light by bombarding a phosphor-coated surface with electrons. Such a cathode-ray tube

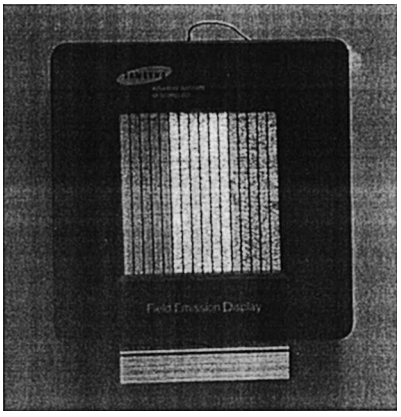

Fig. 11. The Samsung 4.5 in. full-color nanotube display. The photograph is courtesy of Dr. Choi, Display Laboratory, Samsung Advanced Institute of Technology.

(also called ''jumbotron lamp'') has been developed by Saito et al. and is reportedly commercially available [125]. The brightness is typically higher by a factor of 2 as compared to conventional thermoionic lighting elements and can be used for giant outdoor displays [80]. Lifetimes of 8000 h have been demonstrated with such devices [99,126].

Field emitters are also of great interest for microwave amplification [193]. This type of application is very demanding because the current density must be at least 0.1 A/cm^2. Zhou et al. constructed a prototype based on a SWNT cathode that is able to reach that lower limit to operate in microwave tubes [194,195].

The same group realized a gas discharge tube that serves as an overvoltage protection [196]. When the voltage between a nanotube cathode and a counter-electrode reaches a threshold value for field emission, the emitted current induces a discharge in the noble gas-filled interelectrode gap. It could be demonstrated that this device shows better performance than commercially available elements.

All these achievements underline the potential of carbon nanotube emitters in applications. Nevertheless, the lack of information on some aspects of device realization like device lifetime, fabrication yield and cost show the demand for more studies. Finally, nearly all devices mentioned work in diode configuration. One of the future challenges is hence the fabrication of gated nanotube devices.

7. Conclusion

What is the state of the art after these five years of research on field emission from carbon nanotubes? It is proven that nanotubes are excellent electron sources, providing a stable current at very low fields and capable of operating in moderate vacuum. Different methods are available to deposit various types of nanotubes on surfaces. Techniques have been developed to pattern the films, to vary the density of nanotubes and their orientation on the substrate and therefore to control their emission properties. It is further possible to place and manipulate one single nanotube on a support. Different properties have been measured, the workfunction has been estimated, and emission models have been proposed.

Despite the fast-paced evolution of the field there are numerous gaps in our understanding. Are localized cap states truly involved in the emission? Do adsorbates really play the central role? Are other, yet unrecognized phenomena involved? These questions will only be answered through detailed studies and comparative experiments where great care is taken to control the physical and chemical state of the emitters. These must include a thorough characterization of the electronic properties of the tube cap and of their influence on the emission. Questions related to the problem of electrical contacts between nanotubes and support will have to be addressed. The degradation remains also a big unknown in spite of its utmost importance for applications. Finally, synthesis and emitter fabrication will remain one of the great issues in future. Is it possible to grow nanotubes at low temperatures? Is the incorporation of nanotubes in gated devices technologically possible? The evolution of the field will be determined to a large extent by the answers to these questions.

It remains, however, that tremendous progress has been achieved during the last five years. If the field continues to develop at the present pace, we can expect reliable and reproducible preparation methods, a better understanding of the emission mechanism and the electronic properties of nanotubes, the demonstration of additional original devices, and hopefully a nanotube FED in our offices in a few years.

Acknowledgements

The work presented in Figs. 2–10 of this article was performed in close collaboration with the members of our respective groups. At the Ecole Polytechnique Fédérale in Lausanne, André Chatelain, Walt A. De Heer (now at Georgia Tech, Atlanta, USA), László Forró, Klara Hernadi (visiting from University of Szeged, Hungary), Klaus Kern, Frédéric Maier, Jean-Paul Salvetat (now at CNRS-CRMD in Orléans, France) and Nicolas Weiss participated in the film preparation, CVD growth, structuration of nanotube films, and in the various studies on field emission on single tubes and nanotube films. At the University in Fribourg, Chris-

toph Emmenegger, Oliver Gröning, Olivier Küttel, Eliane Schaller and Louis Schlapbach participated in the FE scanning measurements on the patterned films. We acknowledge gratefully the precious contributions of all our coworkers. We thank also Dr Choi from the Display Lab of the Samsung Advanced Institute of Technology for making the photograph of the display reproduced in Fig. 11 available. The electron microscopy was performed at the Centre Interdépartemental de Microscopie Electronique of EPFL. Financial support was provided in part by the Swiss National Science Foundation.

References

[1] Iijima S. Nature 1991;354:56.
[2] Hamada N, Sawada S-I, Oshiyama A. Phys Rev Lett 1992;68:1579.
[3] Saito R, Fujita M, Dresselhaus G, Dresselhaus MS. Appl Phys Lett 1992;60:2204.
[4] Wildoer JWG, Venema LC, Rinzler AG, Smalley RE, Dekker C. Nature 1998;391:59.
[5] Odom TW, Lin HJ, Kim P, Lieber CM. Nature 1998;391:62.
[6] Treacy MMJ, Ebbesen TW, Gibson JM. Nature 1996;381:678.
[7] Falvo MR, Clary GJ, Taylor II RM, Chi V, Brooks Jr FP, Washburn S, Superfine R. Nature 1997;389:582.
[8] Wong EW, Sheehan PE, Lieber CM. Science 1997;277:1971.
[9] Salvetat J-P, Kulik AJ, Bonard J-M, Briggs GAD, Stöckli T, Méténier K, Bonnamy S, Béguin F, Burnham NA, Forró L. Adv Mater 1999;11:161.
[10] Salvetat J-P, Briggs GAD, Bonard J-M, Bacsa RR, Kulik AJ, Stöckli T, Burnham NA, Forró L. J Phys Rev Lett 1999;82:944.
[11] Yu M-F, Lourie O, Dyer MJ, Moloni K, Kelly TF, Ruoff RS. Science 2000;287:637.
[12] Andrews R, Jacques D, Rao AM, Rantell T, Derbyshire F, Chen Y, Chen J, Haddon RC. Appl Phys Lett 1999;75:1329.
[13] Laurent C, Peigney A, Dumortier O, Rousset A. J Eur Ceram Soc 1998;18:2005.
[14] Tans SJ, Verschueren RM, Dekker C. Nature 1998; 393:49.
[15] Martel R, Schmidt T, Shea HR, Hertel T, Avouris P. Appl Phys Lett 1998;73:2447.
[16] Roschier L, Penttila J, Martin M, Hakonen P, Paalanen M, Tapper U, Kauppinen EI, Journet C, Bernier P. Appl Phys Lett 1999;75:728.
[17] Dai H, Hafner JH, Rinzler AG, Colbert DT, Smalley RE. Nature 1996;384:147.
[18] Cooper EB, Manalis SR, Fang H, Dai H, Matsumoto K, Minne SC, Hunt T, Quate CF. Appl Phys Lett 1999;75:3566.
[19] Kong J, Franklin NR, Zhou C, Chapline MG, Peng S, Cho K, Dai H. Science 2000;287:622.
[20] Wong SS, Joselevich E, Woolley AT, Li CC, Lieber CM. Nature 1998;394:52.
[21] Wong SS, Woolley AT, Joselevich E, Lieber CM. Chem Phys Lett 1999;306:5.
[22] Chernozatonskii LA, Gulyaev YV, Kosakovskaya ZY, Sinitsyn NI, Torgashov GV, Zakharchenko YF, Fedorov EA, Val'chuk VP. Chem Phys Lett 1995; 233:63.
[23] Rinzler AG, Hafner JH, Nikolaev P, Lou L, Kim SG, Tomanek D, Nordlander P, Colbert DT, Smalley RE. Science 1995;269:1550.
[24] De Heer WA, Châtelain A, Ugarte D. Science 1995;270:1179.
[25] Ebbesen TW. Phys Today 1996;49:26.
[26] Ajayan PM, Ebbesen TW. Rep Prog Phys 1997;60:1025.
[27] Yakobson BI, Smalley RE. Am Sci 1997;85:324.
[28] Dekker C. Phys Today 1999;52:22.
[29] Dresselhaus MS, Dresselhaus G, Eklund PC. Science of fullerenes and carbon nanotubes. New York: Academic Press; 1996.
[30] Ebbesen TW. Carbon nanotubes: preparation and properties. Boca Raton, FL: CRC Press; 1997.
[31] Tanaka K, Yamabe T, Fukui K. The science and technology of carbon nanotubes. Amsterdam: Elsevier; 1999.
[32] Bernaerts D, Op De Beeck M, Amelinckx S, Van Landuyt J, Van Tendeloo G. Phil Mag A 1996;74:723.
[33] Zhang XF, Zhang XB, van Tendeloo G, Amelinckx S, Op de Beeck M, van Landuyt J. J Cryst Growth 1993; 130:3.
[34] Iijima S, Ichihashi T, Ando Y. Nature 1992;356:777.
[35] Chico L, Crespi VH, Benedict LX, Louie SG, Cohen ML. Phys Rev Lett 1996;76:971.
[36] Blase X, Benedict LX, Shirley EL, Louie SG. Phys Rev Lett 1994;72:1878.
[37] Mintmire JW, White CT. Carbon 1995;33:893.
[38] Kane CL, Mele EJ. Phys Rev Lett 1997;78:1932.
[39] Wallace PR. Phys Rev 1947;71:622.
[40] Venema LC, Wildoer JWG, Dekker C, Rinzler AG, Smalley RE. Appl Phys A 1998;66:1.
[41] Odom TW, Huang J-L, Kim P, Lieber CM. J Phys Chem B 2000;104:2794.
[42] Venema LC, Wildoer JWG, Janssen JW, Tans SJ, Tuinstra HLJT, Kouwenhoven LP, Dekker C. Science 1999;283:52.
[43] Kim P, Odom TW, Lin HJ, Lieber CM. Phys Rev Lett 1999;82:1225.
[44] Bockrath M, Cobden DH, McEuen PL, Chopra NG, Zettl A, Thess A, Smalley RE. Science 1997;275: 1922.
[45] Tans SJ, Devoret MH, Dai H, Thess A, Smalley RE, Georliga LJ, Dekker C. Nature 1997;386:474.
[46] Tans SJ, Devoret MH, Groeneveld RJA, Dekker C. Nature 1998;394:761.
[47] Bockrath M, Cobden DH, Jia L, Rinzler AG, Smalley RE, Balents L, McEuen PL. Nature 1999;397:598.
[48] Bachtold A, Strunk C, Salvetat J-P, Bonard J-M, Forró L, Nussbaumer T, Schönenberger C. Nature 1999; 397:673.
[49] Soh HT, Quate CF, Morpurgo AF, Marcusa CM, Kong J, Dai H. Appl Phys Lett 1999;75:627.
[50] Schönenberger C, Bachtold A, Strunk C, Salvetat J-P, Forró L. Appl Phys A 1999;69:283.

[51] Kong J, Zhou C, Morpurgo A, Soh HT, Quate CF, Marcus C, Dai H. Appl Phys A 1999;69:305.
[52] Kun L, Burghard M, Roth S, Bernier P. Appl Phys Lett 1999;75:2494.
[53] McEuen PL, Bockrath M, Cobden DH, Yoon YG, Louie SG. Phys Rev Lett 1999;83:5098.
[54] Dai H, Wong EW, Lieber CM. Science 1996;272:523.
[55] Langer L, Bayot V, Grivei E, Issi JP, Heremans JP, Olk CH, Stockman L, Van Haesendonck C, Bruynseraede Y. Phys Rev Lett 1996;76:479.
[56] Ebbesen TW, Lezec HJ, Hiura H, Bennett JW, Ghaemi HF, Thio T. Nature 1996;382:54.
[57] Jie H, Anantram MP, Jaffe RL, Kong J, Dai H. Phys Rev B 1998;57:14983.
[58] Crespi VH. Phys Rev B 1998;58:12671.
[59] Lambin P, Meunier V. Appl Phys A 1999;68:263.
[60] Yao Z, Postma HWC, Balents L, Dekker C. Nature 1999;402:273.
[61] Bachtold A, Henny M, Terrier C, Strunk C, Schönenberger C, Salvetat J-P, Bonard J-M, Forró L. Appl Phys Lett 1998;73:274.
[62] Tersoff J. Appl Phys Lett 1999;74:2122.
[63] Ebbesen TW, Ajayan PM. Nature 1992;358:220.
[64] Iijima S, Ichihashi T. Nature 1993;363:603.
[65] Bethune DS, Kiang CH, de Vries MS, Gorman G, Savoy R, Vazquez J, Beyers R. Nature 1993;363:605.
[66] Abrahamson J, Wiles PG, Rhoades BL. Carbon 1999;37:1874 originally published in 1979.
[67] Thrower PA. Carbon 1999;37:1677.
[68] Wang XK, Lin XW, Dravid VP, Ketterson JB, Chang RPH. Appl Phys Lett 1995;66:2430.
[69] Maser WK, Lambert JM, Ajayan PM, Stephan O, Bernier P. Synthetic Metals 1996;77:1.
[70] Journet C, Bernier P. Appl Phys A 1998;67:1.
[71] Thess A, Lee R, Nikolaev P, Dai H, Petit P, Robert J, Chunhui X, Hee LY, Gon KS, Rinzler AG, Colbert DT, Scuseria GE, Tomanek D, Fischer JE, Smalley RE. Science 1996;273:483.
[72] Rinzler AG, Liu J, Dai H, Nikolaev P, Huffman CB, Macias FJR, Boul PJ, Lu AH, Heymann D, Colbert DT, Lee RS, Fischer JE, Rao AM, Eklund PC, Smalley RE. Appl Phys A 1998;67:29.
[73] Walker Jr PL, Rakszawski JF, Imperial GR. J Phys Chem 1959;63:133.
[74] Dresselhaus MS, Dresselhaus G, Sugihara K, Spain IL, Goldberg HA. Graphite fibers and filaments. Berlin: Springer; 1988.
[75] Kim MS, Rodriguez NM, Baker RTK. J Catal 1991;131:60.
[76] Oberlin A, Endo M. J Cryst Growth 1976;94:834.
[77] Tibbetts GG. J Cryst Growth 1984;66:632.
[78] José-Yacaman M, Miki-Yoshida M, Rendón L, Santiesteban JG. Appl Phys Lett 1993;62:657.
[79] de Pablo PJ, Howell S, Crittenden S, Walsh B, Graugnard E, Reifenberger R. Appl Phys Lett 1999;75:3941.
[80] Bonard J-M, Salvetat J-P, Stöckli T, Forró L, Châtelain A. Appl Phys A 1999;69:245.
[81] Saito Y, Hamaguchi K, Uemura S, Uchida K, Tasaka Y, Ikazaki F, Yumura M, Kasuya A, Nishina Y. Appl Phys A 1998;67:95.
[82] Endo M, Takeuchi K, Igarashi S, Kobori K, Shiraishi M, Kroto HW. J Phys Chem Sol 1993;54:1841.
[83] Ivanov V, Nagy JB, Lambin P, Lucas A, Zhang XB, Zhang XF, Bernaerts D, Van Tendeloo G, Amelinckx S, Van Landuyt J. Chem Phys Lett 1994;223:329.
[84] Hernadi K, Fonseca A, Nagy JB, Bernaerts D, Riga J, Lucas A. Synthetic Metals 1996;77:1.
[85] Fonseca A, Hernadi K, Piedigrosso P, Colomer JF, Mukhopadhyay K, Doome R, Lazarescu S, Biro LP, Lambin P, Thiry PA, Bernaerts D, Nagy JB. Appl Phys A 1998;67:11.
[86] Nikolaev P, Bronikowski MJ, Bradley K, Rohmund F, Colbert DT, Smith KA, Smalley RE. Chem Phys Lett 1999;313:1.
[87] Kong J, Cassell AM, Dai H. Chem Phys Lett 1998;292:567.
[88] Li WZ, Xie SS, Qian LX, Chang BH, Zou BS, Zhou WY, Zhao RA, Wang G. Science 1996;274:1701.
[89] Pan ZW, Xie SS, Chang BH, Sun LF, Zhou WY, Wang G. Nature 1998;394:631.
[90] Terrones M, Grobert N, Olivares J, Zhang JP, Terrones H, Kordatos K, Hsu WK, Hare JP, Townsend PD, Prassides K, Cheetham AK, Kroto HW, Walton DRM. Nature 1997;388:52.
[91] Küttel OM, Gröning O, Emmenegger C, Schlapbach L. Appl Phys Lett 1998;73:2113.
[92] Ren ZF, Huang ZP, Xu JW, Wang JH, Bush P, Siegal MP, Provencio PN. Science 1998;282:1105.
[93] Fan S, Chapline MG, Franklin NR, Tombler TW, Cassell AM, Dai H. Science 1999;283:512.
[94] Lee CJ, Kim DW, Lee TJ, Choi YC, Park YS, Lee YH, Choi WB, Lee NS, Park GS, Kim JM. Chem Phys Lett 1999;312:5.
[95] Araki H, Kajii H, Yoshino K. Jpn J Appl Phys 1999;38:L836.
[96] Kind H, Bonard J-M, Emmenegger C, Nilsson L-O, Hernadi K, Maillard-Schaller E, Schlapbach L, Forró L, Kern K. Adv Mater 1999;11:1285.
[97] Choi YC, Bae DJ, Lee YH, Lee BS, Han IT, Choi WB, Lee NS, Kim JM. Synthetic Metals 2000;108:159.
[98] Chen Y, Shaw DT, Guo L. Appl Phys Lett 2000;76:2469.
[99] Murakami H, Hirakawa M, Tanaka C, Yamakawa H. Appl Phys Lett 2000;76:1776.
[100] Li J, Papadopoulos C, Xu JM, Moskovits M. Appl Phys Lett 1999;75:367.
[101] Davydov DN, Sattari PA, AlMawlawi D, Osika A, Haslett L, Moskovits M. J Appl Phys 1999;86:3983.
[102] Ebbesen TW, Ajayan PM, Hiura H, Tanigaki K. Nature 1994;367:519.
[103] Tsang SC, Chen YK, Harris PJF, Green MLH. Nature 1994;372:159.
[104] Hiura H, Ebbesen TW, Tanigaki K. Adv Mater 1995;7:275.
[105] Colbert DT, Zhang J, McClure SM, Nikolaev P, Chen Z, Hafner JH, Owens DW, Kotula PG, Carter CB, Weaver JH, Rinzler AG, Smalley RE. Science 1994;266:1218.
[106] Ugarte D, DeHeer WA, Châtelain A. Science 1996;274:1897.
[107] Dujardin E, Ebbesen TW, Krishnan A, Treacy MMJ. Adv Mater 1998;10:611.

[108] Bonard J-M, Stora T, Salvetat J-P, Maier F, Stöckli T, Duschl C, Forró L, De Heer WA, Châtelain A. Adv Mater 1997;9:827.
[109] Duesberg GS, Burghard M, Muster J, Philipp G, Roth S. Chem Commun 1998;8:435.
[110] Bandow S, Rao AM, Williams KA, Thess A, Smalley RE, Eklund PC. J Phys Chem B 1997;101:8839.
[111] Duesberg GS, Muster J, Krstic V, Burghard M, Roth S. Appl Phys A 1998;67:117.
[112] Fransen MJ, van Rooy TL, Kruit P. Appl Surf Sci 1999;146:312.
[113] Bonard J-M, Maier F, Stöckli T, Châtelain A, De Heer WA, Salvetat J-P, Forró L. Ultramicroscopy 1998;73:9.
[114] Schmid H, Fink H-W. Appl Phys Lett 1997;70:2679.
[115] Saito Y, Hamaguchi K, Hata K, Tohji K, Kasuya A, Nishina Y, Uchida K, Tasaka Y, Ikazaki F, Yumura M. Ultramicroscopy 1998;73:1.
[116] Lovall D, Buss M, Graugnard E, Andres RP, Reifenberger R. Phys Rev B 2000;61:5683.
[117] Dean KA, Chalamala BR. Appl Phys Lett 1999;75:3017.
[118] Spindt CA, Brodie I, Humphtey L, Westerberg ER. J Appl Phys 1976;47:5248.
[119] De Heer WA, Bacsa WS, Châtelain A, Gerfin T, Humphrey Baker R, Forró L, Ugarte D. Science 1995;268:845.
[120] Bonard J-M, Salvetat J-P, Stöckli T, De Heer WA, Forró L, Châtelain A. Appl Phys Lett 1998;73:918.
[121] Bower C, Zhou O, Zhu W, Ramirez AG, Kochanski GP, Jin S. Mater Res Soc Symp Proc, in press.
[122] Fishbine BH, Miglionico CJ, Hackett KE, Hendricks K. J Mater Res Soc Symp Proc 1994;349:319.
[123] Fishbine BH, Miglionico CJ, Hackett KE, Hendricks KJ, Wang XK, Chang RPH, Shovlin JD, Kordesch ME. Mater Res Soc Symp Proc 1995;359:319.
[124] Collins PG, Zettl A. Appl Phys Lett 1996;69:1969.
[125] Saito Y, Uemura S, Hamaguchi K. Jpn J Appl Phys 1998;37:L346.
[126] Saito Y, Uemura S. Carbon 2000;38:169.
[127] Wang QH, Setlur AA, Lauerhaas JM, Dai JY, Seelig EW, Chang RPH. Appl Phys Lett 1998;72:2912.
[128] Choi WB, Chung DS, Kang JH, Kim HY, Jin YW, Han IT, Lee YH, Jung JE, Lee NS, Park GS, Kim JM. Appl Phys Lett 1999;75:3129.
[129] Chung DS, Choi WB, Kang JH, Kim HY, Han IT, Park YS, Lee YH, Lee NS, Jung JE, Kim JM. J Vac Sci Technol 2000;B18:1054.
[130] Ahlskog M, Seynaeve E, Vullers RJM, Van Haesendonck C. J Appl Phys 1999;85:8432.
[131] Burghard M, Duesberg G, Philipp G, Muster J, Roth S. Adv Mater 1998;10:584.
[132] Liu J, Casavant MJ, Cox M, Walters DA, Boul P, Wei L, Rimberg AJ, Smith KA, Colbert DT, Smalley RE. Chem Phys Lett 1999;303:1.
[133] Terrones M, Grobert N, Zhang JP, Terrones H, Olivares J, Hsu WK, Hare JP, Cheetham AK, Kroto HW, Walton DRM. Chem Phys Lett 1998;285:299.
[134] Xu X, Brandes GR. Appl Phys Lett 1999;74:2549.
[135] Ren ZF, Huang ZP, Wang DZ, Wen JG, Xu JW, Wang JH, Calvet LE, Chen J, Klemic JF, Reed MA. Appl Phys Lett 1999;75:1086.
[136] Yang Y, Huang S, He H, Mau AWH, Dai L. J Am Chem Soc 1999;121:10832.
[137] Huang S, Dai L, Mau AWH. J Phys Chem B 1999;103:4223.
[138] Kumar A, Whitesides GM. Appl Phys Lett 1993;63:2002.
[139] Cassell AM, Raymakers JA, Kong J, Dai H. J Phys Chem B 1999;103:6484.
[140] Kind H, Bonard J-M, Forró L, Kern K, Hernadi K, Nilsson L-O, Schlapbach L. Langmuir 2000;16:6877.
[141] Cassell AM, Franklin NR, Tombler TW, Chan EM, Han J, Dai H. J Am Chem Soc 1999;121:7975.
[142] Dai H, Kong J, Zhou C, Franklin N, Tombler T, Cassell A, Fan S, Chapline M. J Phys Chem B 1999;103:11246.
[143] Franklin NR, Dai H. Adv Mater 2000;12:890.
[144] Huang S, Mau AWH, Turney TW, White PA, Dai L. J Phys Chem B 2000;104:2193.
[145] Good RH, Müller EW. Handbuch der Physik 1956;21:176.
[146] Dyke WP, Dolan WW. Adv Electron El Phys 1956;8:89.
[147] Gadzuk JW, Plummer EW. Rev Mod Phys 1973;45:487.
[148] Modinos A. Field, thermoionic, and secondary electron spectroscopy. New York: Plenum Publishing Corporation; 1984.
[149] Gomer R. Surf Sci 1994;299/300:129.
[150] Chernozatonskii LA, Kosakovskaja ZJ, Kiselev AN, Kiselev NA. Chem Phys Lett 1994;228:1.
[151] Chernozatonskii LA, Gulyaev YV, Kosakovskaya Z, Sinitsyn NI, Torgashov GV, Fedorov EA, Zakharchenko YF, Val'chuk VP. Mater Res Soc Symp Proc 1995;359:99.
[152] Chernozatonskii LA, Kosakovskaya Z, Gulyaev YV, Sinitsyn NI, Torgashov GV, Zakharchenko YF. J Vac Sci Technol B 1996;14:2080.
[153] Sinitsyn NI, Gulyaev YV, Torgashov GV, Chernozatonskii LA, Kosakovskaya Z, Zakharchenko YF, Kiselev NA, Musatov AL, Zhbanov AI, Mevlyut ST, Glukhova OE. Appl Surf Sci 1997;111:145.
[154] De Heer WA, Bonard J-M, Stöckli T, Châtelain A, Forró L, Ugarte D. Zeitschrift fur Physik D 1997;40:1.
[155] Wang QH, Corrigan TD, Dai JY, Chang RPH, Krauss AR. Appl Phys Lett 1997;70:3308.
[156] Zhu W, Bower C, Zhou O, Kochanski G, Jin S. Appl Phys Lett 1999;75:873.
[157] Obraztsova ED, Bonard J-M, Kuznetsov VL, Zaikovskii VI, Pimenov SM, Pozarov AS, Terekhov SV, Konov VI, Obraztsov AN, Volkov AS. Nanostructured Mater 1999;12:567.
[158] Obraztsov AN, Volkov AP, Pavlovskii IY, Chuvilin AL, Rudina NA, Kuznetsov VL. JETP Lett 1999;69:411.
[159] Xu D, Guo G, Gui L, Tang Y, Shi Z, Jin Z, Gu Z, Liu W, Li X, Zhang G. Appl Phys Lett 1999;75:481.
[160] Obraztsov AN, Pavlovsky I, Volkov AP, Obraztsova ED, Chuvilin AL, Kuznetsov VL. J Vac Sci Technol B 2000;18:1059.
[161] Rao AM, Jacques D, Haddon RC, Zhu W, Bower C, Jin S. Appl Phys Lett 2000;76:3813.
[162] Ma X, Wang E, Wuzong Z, Jefferson DA, Jun C, Shaozhi D, Ningsheng X, Jun Y. Appl Phys Lett 1999;75:3105.
[163] Küttel OM, Gröning O, Emmenegger C, Nilsson L, Maillard E, Diederich L, Schlapbach L. Carbon 1999;37:745.

[164] Dimitrijevic S, Withers JC, Mammana VP, Monteiro OR, Ager JW, Brown III IG. Appl Phys Lett 1999;75:2680.
[165] Bonard J-M, Weiss N, Kind H, Stöckli T, Forró L, Kern K, Châtelain A. Adv Mater, in press.
[166] Nilsson L, Gröning O, Emmenegger C, Küttel O, Schaller E, Schlapbach L, Kind H, Bonard J-M, Kern K. Appl Phys Lett 2000;76:2071.
[167] Nilsson L, Gröning O, Emmenegger C, Küttel O, Schaller E, Schlapbach L, Kind H, Bonard J-M, Kern K. in preparation.
[168] Poncharal P, Wang ZL, Ugarte D, De Heer WA. Science 1999;283:1513.
[169] Rinzler AG, Hafner JK, Colbert DT, Smalley RE. Mat Res Soc Symp Proc 1995;359:61.
[170] Collins PG, Zettl A. Phys Rev B 1997;55:9391.
[171] Dean KA, Chalamala BR. Appl Phys Lett 2000;76:375.
[172] De Heer WA, Poncharal P, Wang ZL. 14th International Winterschool on Electronic Properties of Novel Mater (IWEPNM2000), Kirchberg, Austria, 4–11 March, 2000.
[173] Wang ZL, Poncharal P, De Heer WA. Microsc Microanal 2000;6:224.
[174] Cumings A, Zettl A. Science 2000;289:602.
[175] Saito Y, Hamaguchi K, Hata K, Tasaka Y, Ikasaki F, Yumura M, Kasuya A, Nishina Y. Nature 1997;389:554.
[176] Saito Y, Hamaguchi K, Nishino T, Iiata K, Tohji K, Kasuya A, Nishina Y. Jpn J Appl Phys 1997;36:L1340.
[177] De Heer WA, Bonard J-M, Fauth K, Châtelain A, Forró L, Ugarte D. Adv Mater 1997;8:87.
[178] Chalamala BR. J Appl Phys 1999;85:3832.
[179] Purcell ST, Binh VT, Garcia N. Appl Phys Lett 1995;67:436.
[180] Dean KA, Gröning O, Küttel OM, Schlapbach L. Appl Phys Lett 1999;75:2773.
[181] Gröning O, Küttel OM, Gröning P, Schlapbach L. J Vac Sci Technol B 1999;17:1064.
[182] Ramprasad R, von Allmen P, Fonseca LRC. Phys Rev B 1999;60:6023.
[183] Ago H, Kugler T, Cacialli F, Salaneck WR, Shaffer MSP, Windle AH, Friend RHJ. Phys Chem B 1999;103:8116.
[184] Bonard J-M, Stöckli T, Maier F, De Heer WA, Châtelain A, Salvetat J-P, Forró L. Phys Rev Lett 1998;81:1441.
[185] Tamura R, Tsukada M. Phys Rev B 1995;52:6015.
[186] Carroll DL, Redlich P, Ajayan PM, Charlier JC, Blase X, De A, Vita R. Phys Rev Lett 1997;78:2811.
[187] De Vita A, Charlier J-C, Blase X, Car R. Appl Phys A 1999;68:283.
[188] Dean KA, von Allmen P, Chalamala BR. J Vac Sci Technol B 1999;17:1959.
[189] Fink H-W, Stocker W, Schmid H. Phys Rev Lett 1990;56:1204.
[190] Fransen MJ. Towards high-brightness, monochromatic electron sources. Delft University of Technology, 1998.
[191] Choi WB, Chung DS, Kang JH, Kim HY, Jin YW, Han IT, Lee YH, Jung JE, Lee NS, Park GS, Kim JM. EuroFE'99 meeting, Toledo, Spain, 15–19 November, 1999.
[192] Kim JM, Lee NS, Choi WB, Jung JE, Han IT, Jung DS, Park SH, Hong SS, Kim HY. 14th International Winterschool on Electronic Properties of Novel Mater. (IWEPNM2000), Kirchberg, Austria, 4–11 March, 2000.
[193] Jensen KL. Phys Plasma 1999;6:2241.
[194] Zhou O. 14th International Winterschool on Electronic Properties of Novel Mater. (IWEPNM2000), Kirchberg, Austria, 4–11 March, 2000.
[195] Zhou O. et al. (UNC Chapel Hill), Zhu W. (Lucent Technologies), pending US patents.
[196] Rosen R, Simendinger W, Debbault C, Shimoda H, Fleming L, Stoner B, Zhou O. Appl Phys Lett 2000;76:1663.
[197] Brandbyge M. Atomic and electronic structure of carbon nanotubes – a notebook for Mathematica. http://www.mathsource.com/MathSource/Applications/Material-Science/0210-463/nanotubes.nb 1999.